Collagen and Leather

REVIEW

Open Access

# Recent advances in metal organic frameworks for the catalytic degradation of organic pollutants

Jinhui Wei[1], Min Yuan[2], Songtao Wang[3], Xuehu Wang[4], Nan An[1], Guangping Lv[1*] and Lina Wu[1*]

**Abstract**

Metal organic frameworks (MOFs) with their large surface area and numerous active sites have attracted significant research attention. Recently, the application of MOFs for the catalytic degradation of organic pollutants has provided effective solutions to address diverse environmental problems. In this review, the latest progress in MOF-based removal and degradation of organic pollutants is summarized according to the different roles of MOFs in the removal reaction systems, such as physical adsorbents, enzyme-immobilization carriers, nanozymes, catalysts for photocatalysis, photo-Fenton and sulfate radical based advanced oxidation processes (SR-AOPs). Finally, the opportunities and challenges of developing advanced MOFs for the removal of organic pollutants are discussed and anticipated.

**Keywords** Metal–organic frameworks (MOFs), Organic pollutants, Catalysis degradation, Removal

*Correspondence:
Guangping Lv
guangpinglyu@njnu.edu.cn
Lina Wu
wuln@njnu.edu.cn
Full list of author information is available at the end of the article

**Graphical Abstract**

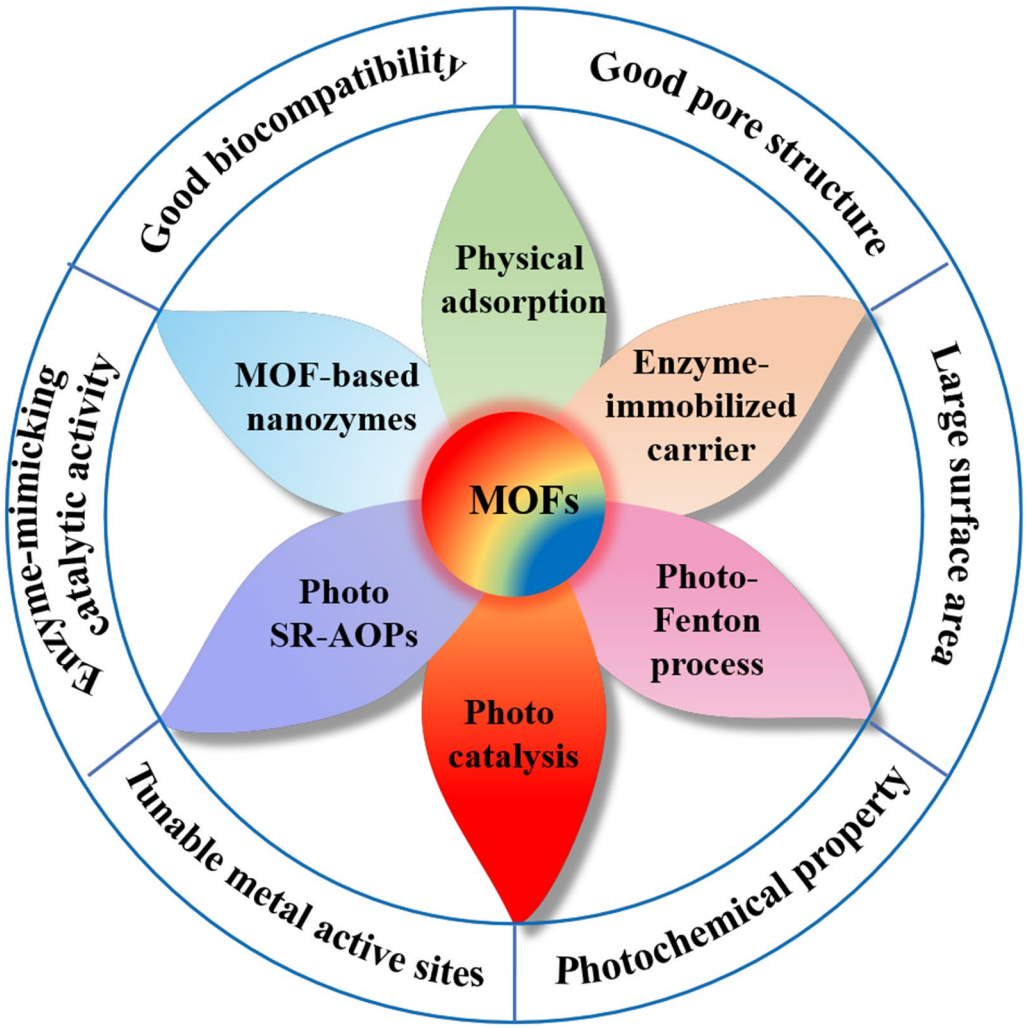


## 1 Introduction

Common organic pollutants include dyes, pesticides, antibiotics and mycotoxins, some of which can pose a severe threat to the environment and human health [1–3]. Notably, mycotoxins produced as secondary metabolites by some fungi have multiple toxic effects on humans and livestock [4]. In addition, pesticides such as herbicides, insecticides and bactericides can also affect the environment and cause health problems [5]. Similarly, antibiotics are a class of drugs that treat infectious diseases in humans. However, the abuse of antibiotics is causing an increase in resistant bacteria [6], as well as metabolic and endocrine disruption. In addition, some dyes are also toxic and are the most commonly seen organic pollutants in the textile and leather industries. Therefore, there has been an increasing concern regarding purifying organic pollutants due to the various recalcitrant pollutants in wastewater from leather production.

Diverse methods have been involved in the removal of organic pollutants, such as physical removal, biodegradation and chemical degradation [7, 8]. Physical methods can separate organic pollutants from the environment and food matrix, but can cause secondary pollution [9]. Biodegradation based on single or combined cultures of bacteria, molds, yeasts, algae, or enzymes, is a popular remediation technique because it is highly economical and environmentally friendly [10, 11]. Although most organic pollutants can be removed by biodegradation [12, 13], some are highly recalcitrant and require additional chemical treatment. In chemical degradation,

advanced oxidation processes (AOPs) have received significant attention, commonly using hydrogen peroxide ($H_2O_2$), hydroxyl radicals (•OH) and sulfate radicals ($SO_4^{\bullet-}$), which can oxidize organic pollutants into less toxic products [14–16]. In addition, Fenton and Fenton-like processes, photocatalysis and $SO_4^{\bullet-}$-based oxidative systems are also examples of AOPs.

Metal organic frameworks (MOFs), formed by the self-assembly of metal ions or metal clusters with organic ligands, have aroused wide attention [17, 18]. The large surface area, numerous adsorption sites [19] and variable functional groups have opened up potential applications of MOFs in catalysis [20], sensing [21], adsorption [22], conductivity [23] and drug delivery [24]. In addition, owing to their high surface areas, optimizable pore volume and pore size distributions, MOFs are becoming a promising class of adsorbents and enzyme immobilization carriers. Due to their tunable metal active sites, MOFs themselves show excellent catalytic performance. Therefore, MOFs have been developed as catalysts for the degradation of organic pollutants in advanced oxidation processes combined with enzyme catalysis and photocatalysis [25–29], while also promoting the adsorption of organic pollutants for effective removal. Several common types of organic pollutants that can be removed by MOFs are listed in Table 1. Consequently, MOFs have proven to be a promising platform for the removal of organic pollutants via physical adsorption, enzyme catalysis and chemical oxidation.

In this article, we provide a comprehensive review of recent findings and developments of MOFs for the removal of organic pollutants, including the fabrication strategies of MOFs and removal mechanisms. The role of MOF microstructures and properties in their catalytic degradation capability are discussed. Also, the strategies for enhancing the performance of pure MOFs to remove organic pollutants are summarized.

## 2 Synthesis of MOFs

MOFs were initially introduced by Omar Yaghi et al. by means of the combination of metal clusters and organic ligands [40]. After that, other types of MOFs such as Materials of Institute Lavoisier (MILs), Zeolitic imidazolate frameworks (ZIFs), University of Oslo (UiO), and PCN developed gradually [41]. MILs are a subclass of MOFs that are fabricated via the coordination of trivalent transition metal ions (such as Fe, Al, and Cr) and carboxylic acid ligands (Fig. 1a) [42, 43]. ZIFs can use transition metal ions to coordinate with imidazolate linkers through self-assembly (Fig. 1b) [44]. Among them, ZIF-8, a typical ZIFs composed of Zn (II) and 2-methylimidazole ligands, found its application as a catalyst in a variety of reactions [45]. Built with the metal center $Zr^{4+}$ and dicarboxylic acid linkers, the UiO family has different ligand lengths but similar network topology, and the strong Zr-O bond coordination is conducive to its stability in various environmental conditions (Fig. 1c) [46]. PCN represents porous coordination network, Ma et al. first designed PCN-9 by a reaction between $H_3$TATB and cobalt nitrate in DMSO [47]. And the reaction between $H_4$adip and Cu $(NO_3)_2$ produced a new MOF designated PCN-14 by Ma and colleagues [48]. Subsequently, with meso-tetra(4-carboxyphenyl) porphyrin (TCPP) as the ligand, more porphyrinic MOFs have been prepared by researchers (Fig. 1d) [49, 50].

Different synthetic approaches were used for the preparation of MOFs, including solvothermal/hydrothermal methods, microwave synthesis, mechanochemical synthesis, sonochemical synthesis and electrochemical synthesis [55–59].

**Table 1** Common organic pollutants that can be removed by MOFs catalysts

| Types | Name | Molecular formula | Hazard | Refs |
|---|---|---|---|---|
| Pesticides | Imidacloprid | $C_9H_{10}ClN_5O_2$ | Eye and skin irritant, liver cell disruption | [30] |
| | Atrazine | $C_8H_{14}ClN_5$ | | [31] |
| | Diazinon | $C_{12}H_{21}N_2O_3PS$ | | [32] |
| | Malathion | $C_{10}H_{19}O_6PS$ | | [32] |
| Antibiotic | Norfloxacin | $C_{16}H_{18}FN_3O_3$ | Liver and kidney issues | [33] |
| | Tetracycline | $C_{22}H_{24}N_2O_8$ | | [34] |
| | Oxytetracycline | $C_{22}H_{24}N_2O_9$ | | [35] |
| Dyes | Methyl orange (MO) | $C_{14}H_{14}N_3SO_3Na$ | Cardiac arrhythmias and vasoconstriction | [36] |
| | Methylene blue (MB) | $C_{37}H_{27}N_3Na_2O_9S_3$ | | [36] |
| Mycotoxins | Deoxynivalenol | $C_{15}H_{20}O_6$ | Carcinogenic and liver damage | [37] |
| | Aflatoxin B1 | $C_{17}H_{12}O_6$ | | [38] |
| | Zearalenone | $C_{18}H_{22}O_5$ | | [39] |

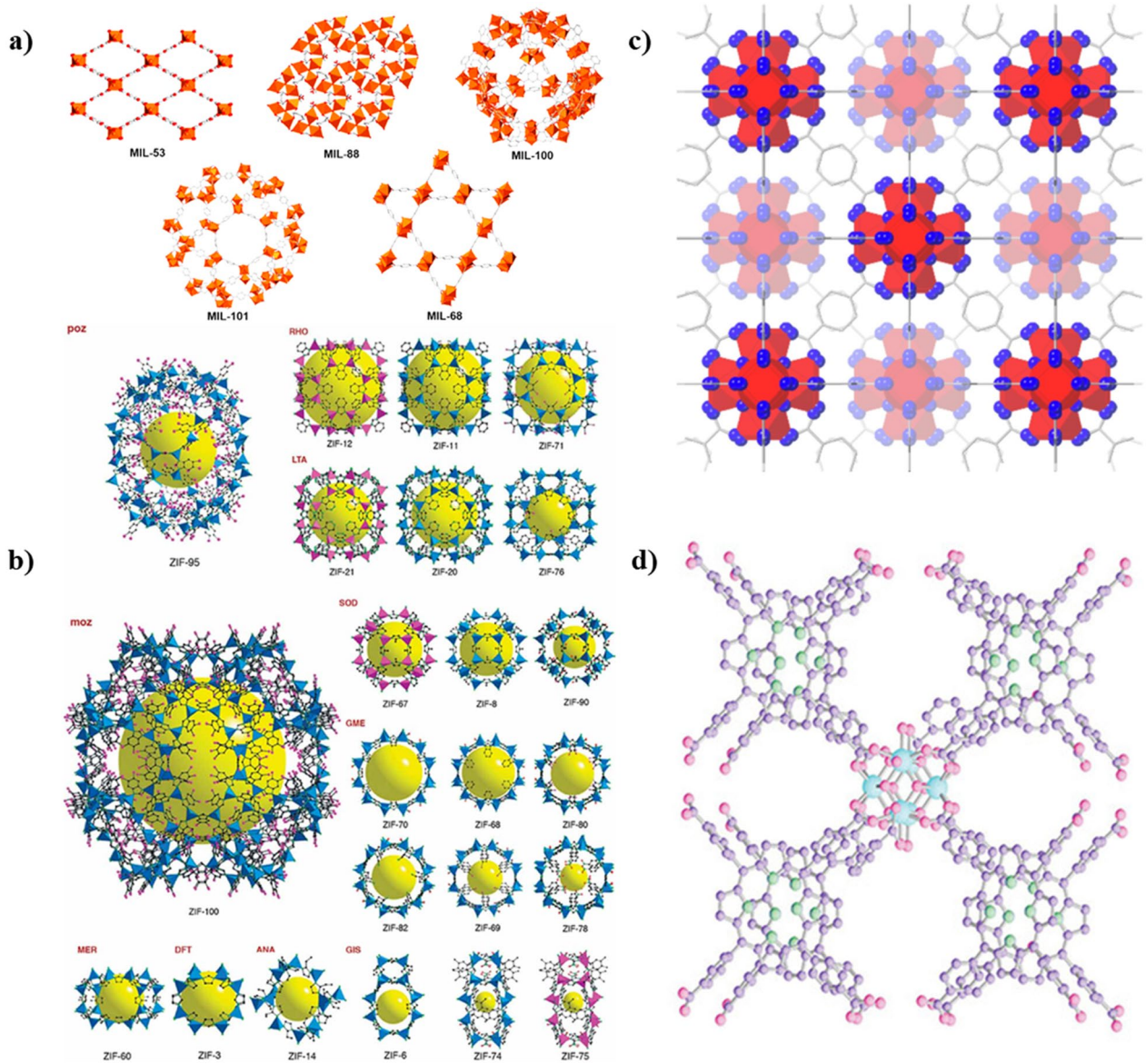


**Fig. 1** **a** Polyhedral structures of MILs [51] (with kind permission from Elsevier) **b** The crystal structure of ZIFs [52] (with kind permission from IOP Publishing Ltd) **c** Tolyhedral representation of the crystal structure of UiO-66 [53] (with kind permission from Elsevier) **d** Crystal structure of PCN-222 [54] (with kind permission from Wiley–VCH)

The most common approach is based on solvothermal/hydrothermal methods (Fig. 2a), which involve the execution of the reaction in an autoclave at a defined temperature [60]. The existing solvothermal methods are based on organic solvents, such as methanol, ethanol, acetone and N,N-dimethylformamide [61]. It is a relatively convenient and facile method, but it has some limitations, including a long reaction time and the high cost of the solvents [62, 63]. To accelerate crystallization and reduce liquid waste, alternative approaches, including electrochemical synthesis, microwave-assisted, mechanochemical and sonochemical, have been developed [64].

Microwave synthesis is a time-saving method, which uses microwave irradiation to heat reactant mixtures in domestic household microwave ovens (DMO) or similar commercially available instrumentation [65, 66]. Using microwave synthesis, various common MOFs such as MIL-101 [67], UiO-66 [68], ZIF-8 [69], PCN-134 [70] (PCN means porous coordination network) and others have been successfully prepared (Fig. 2b).

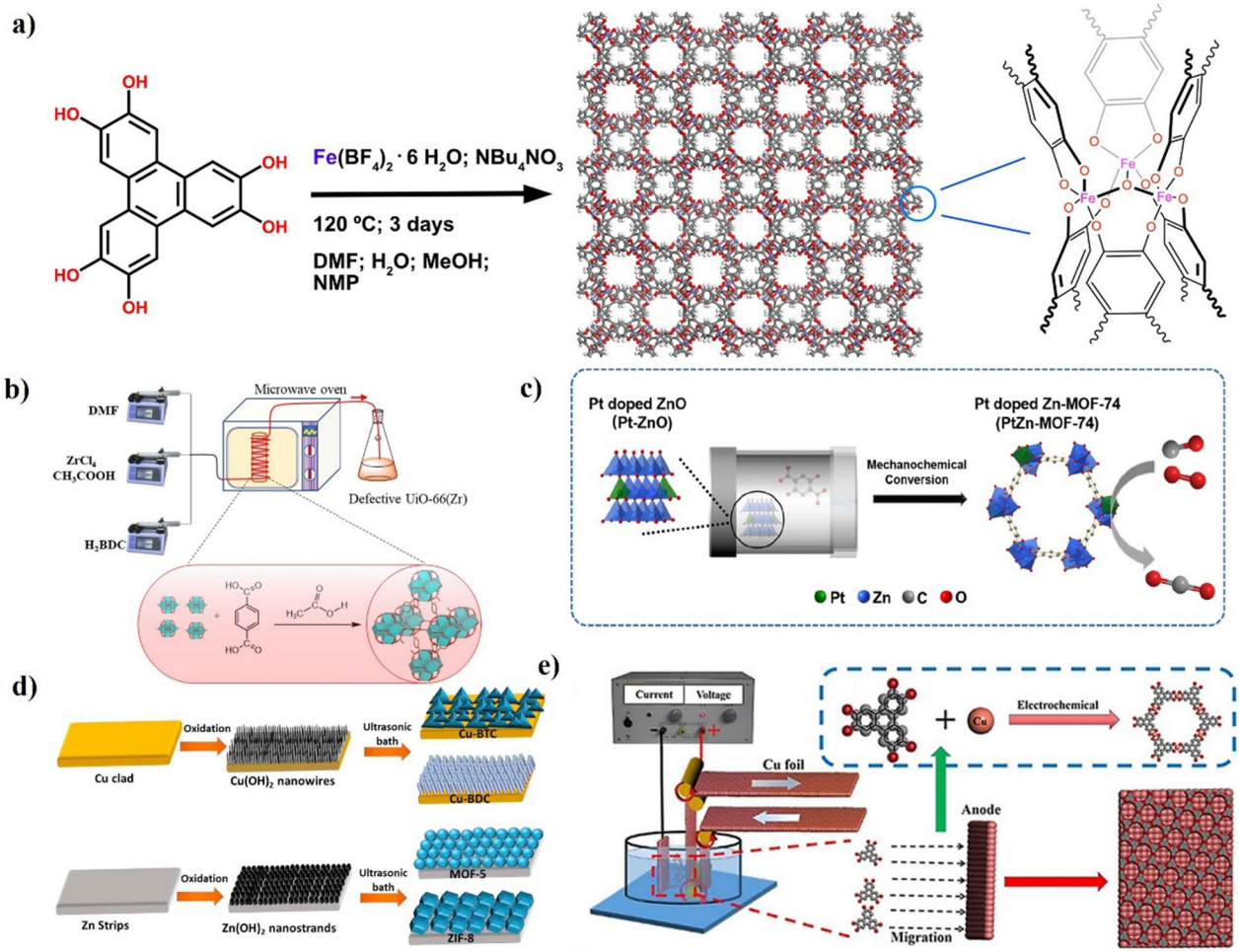


**Fig. 2** **a** Synthesis of MOFs by solvothermal/hydrothermal methods [71] (with kind permission from Wiley–VCH) **b** Microwave synthesis method [72] (with kind permission from Elsevier). **c** Mechanochemical synthesis method [73] (with kind permission from Elsevier) **d** Sonochemical synthesis method [74] (with kind permission from Wiley–VCH) **e** Electrochemical synthesis method [75] (with kind permission from Elsevier)

Mechanochemical synthesis is a green and eco-friendly approach (Fig. 2c), using methods such as ball-milling, screw extrusion, liquid-assisted resonant acoustic mixing and other approaches [76]. This synthesis method has attracted extensive attention because it uses little or no solvents, enables time-saving one pot synthesis, and generates minimal waste [77]. Liquid-assisted grinding (LAG) and ion- or liquid-assisted grinding (ILAG) are the most commonly used methods in mechanochemical synthesis. Compared with absolutely solvent-free approaches, these methods promote the dissolution of solid reagents and improve the formation of coordination bonds [78, 79]. Uzarevic et al. reported the first synthesis of zirconium MOFs (Zr-MOFs) using the LAG method [80]. The catalysis and porosity measurements showed that Zr-MOFs made by LAG had properties comparable to solvothermally synthesized materials.

Sonochemical synthesis uses ultrasound energy ranging from 20 to 1000 kHz, which enables the preparation of numerous MOFs with diverse crystal sizes and morphologies [81–83] (Fig. 2d). In general, the morphology and particle size of MOFs are affected by reaction time, temperature and ultrasonic power. Armstrong et al. optimized HKUST-1 crystals and revealed the crystallization mechanisms by modifying the reaction time and other parameters [84]. Compared with conventional solvothermal/ hydrothermal methods, this method can produce MOFs with homogeneous nucleation centers, while avoiding the need for high temperatures and pressures.

Electrochemical synthesis is a promising method that applies electrical current to chemical synthesis reactions [85] (Fig. 2e). This method can be divided into electrode superficial nucleation (ESN), indirect bipolar electrodeposition (IBED), and electrophoretic deposition (EPD) [86]. In this approach, there is no requirement for metal

salts as precursors because the metal ions are generated by the electrodes [56].

## 3 Strategy for organic pollutants removal

### 3.1 Synergism of physical adsorption to catalytic degradation

Although MOFs are used for catalytic degradation, their adsorption capacity is also an important characteristic for the removal of organic pollutants. Due to their tunable porosities and large surface area, MOFs could remove organic pollutants by adsorption [87]. The removal of organic pollutants by MOFs is facilitated by multiple mechanisms including π-π stacking, electrostatic interactions, hydrogen bonding and acid–alkali interactions [88].

Gao et al. synthesized MIL-53(Cr), MIL-53(Fe) and MIL-53(Al) for sulfamethoxazole (SMZ) removal [89]. The maximum adsorption capacities predicted by a Langmuir model were 468.56, 450.83 and 75.53 $mg{\cdot}g^{-1}$ for MIL-53(Cr), MIL-53(Al), and MIL-53(Fe). The results revealed that metal nodes play an important role in SMZ removal. Zhao et al. reported PCN-222 for chloramphenicol (CAP) removal [90]. PCN-222 exhibited a large adsorption capacity of 370 mg $g^{-1}$ and the adsorption equilibrium could be quickly reached after only 58 s. The large 1-D channels and the abundant hydroxyl groups of PCN-222 could improve the removal efficiency of CAP.

In addition, the introduction of functional groups such as $-NH_2$, $-NO_2$ or $-SO_4$ and doping with metals such as Cu, Co, Mn and Ni could effectively improve the adsorption performance of MOFs [91]. Yu et al. fabricated a variety of porous MOFs, such as MIL-53(Fe), $NH_2$-MIL-53(Fe), $NO_2$-MIL-53(Fe) and Br-MIL-53(Fe) [92]. The maximum adsorption capacities of $NH_2$-MIL-53(Fe), $NO_2$-MIL-53(Fe) and Br-MIL-53(Fe) for the removal of tetracycline (TC) were 271.9 mg $g^{-1}$, 272.6 mg $g^{-1}$ and 309.6 mg $g^{-1}$, which were respectively 9, 10 and 25% higher than the capacity of the pure MIL-53(Fe) (247.7 mg $g^{-1}$) (Fig. 3a). Dehghan et al. compared the TC adsorption capacities of four MOFs (ZIF-67-$NO_3$, ZIF-67-Cl, ZIF-67-$SO_4$ and ZIF-67-OAC) with different chemical groups and four MOFs (ZIF-8-Octahedron, ZIF-8-Leaf, ZIF-8-Cuboid and ZIF-8-Cube) with different structures [93]. ZIF-67-Acetate exhibited the optimal performance (93.7%), showing 2.65 times higher removal efficiency than ZIF-67 (35.3%) (Fig. 3b). Yang et al. fabricated the Mn-doped UiO-66 (MnUiO-66) using solvothermal method for TC removal [94]. Doping with Mn added the active sites of UiO-66 (Fig. 3c). The maximum adsorption capacity of MnUiO-66 was 72.5 $mg{\cdot}g^{-1}$, almost six times higher than that of pure UiO-66. Jin et al. reported MIL-101 nanoparticles co-doped with Cu and Co, and used them as an adsorbent for efficient removal of TC [95]. Compared with pure MIL-101, the adsorption capacity of Cu-Co/MIL-101 was increased by 140% (Fig. 3d). In parallel, the outstanding adsorption performance can cooperate with the catalysis of MOFs for organic pollutants decontamination. For the elimination

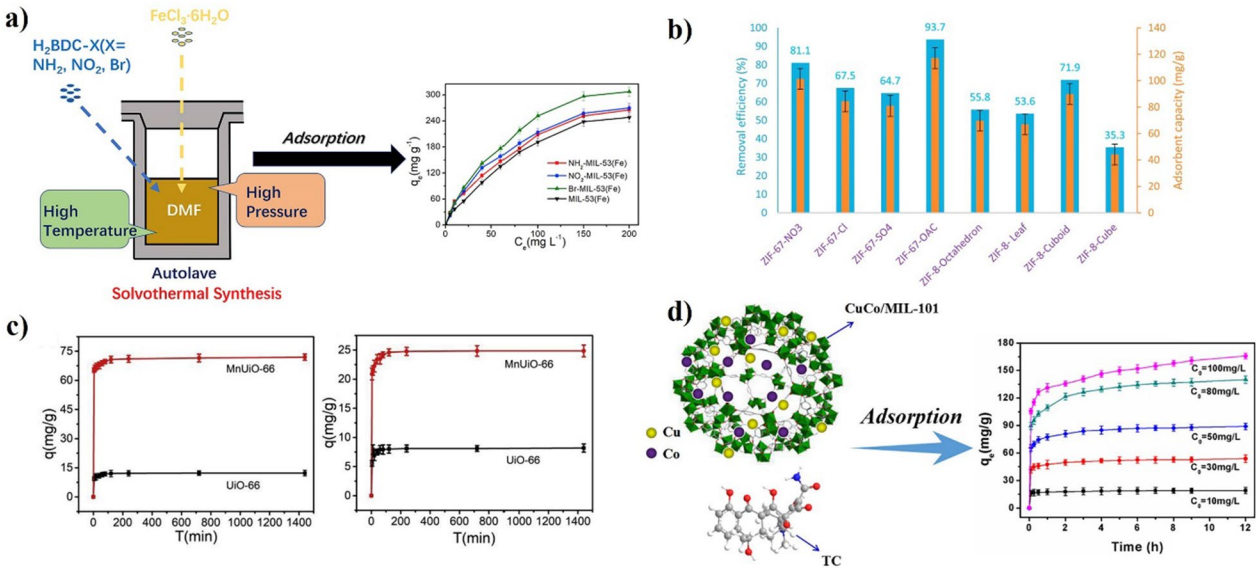


**Fig. 3** **a** The adsorption capacity of MIL-53(Fe)-based MOFs at different equilibrium concentrations [92] (with kind permission from Elsevier) **b** Removal efficiency and adsorption capacity of studied MOFs for TC [93] (with kind permission from Elsevier) **c** Adsorption performance of UiO-66 and MnUiO-66 for TC and Cr(VI) [94] (with kind permission from Elsevier) **d** Adsorption performance of pure MIL-101 and various MNPs/MIL-101 composites [95] (with kind permission from Elsevier)

of dyes in wastewater, a novel Fe-loaded MOF-545(Fe) was synthesized by Zhang et al. [36]. The formed material not only showed high absorption capabilities, but also exhibited POD-like activity, which achieved removing MO and MB in a short period of time (about 2 h). In the case of photocatalysis, Jin et al. [96] synthesized MIL-101(Fe)@MIL-100(Fe) heterojunction to achieve 80% degradation of TC. Owing to the synergistic adsorption between the outer shell and nuclear layer, the Z-scheme heterojunction displayed a pore channel limited effect, which increased TC adsorption quantity and promoted TC photocatalytic properties. Li et al. [97] designed magnetic porous $Fe_3O_4$/carbon octahedra for Fenton-like catalytic removal of organic dye MB, the removal rate can reach nearly 100% in 30 min. The authors observed that the material exhibited excellent Fenton-like catalytic performance with MB molecules first adsorbed on the surface of catalysts, then diffused through mesoporous channels and sparked a Fenton-like reaction. Therefore, the synergistic impact of integrating physical adsorption and catalytic reactions may stimulate unique organic pollutant removal effects.

### 3.2 Enzyme-immobilization carrier assisted enzymatic degradation

Although native enzymes are also used for the degradation of pollutants [98, 99], the fragile nature of native enzymes makes them susceptible to denaturation or instability in extreme environments which results in inactivation and an extremely high cost [100, 101]. Enzyme immobilization was an efficient strategy to improve the activity and stability of native enzymes. Owing to their high specific surface area, porous structure and good biocompatibility, MOFs hold great promise as enzyme immobilization carriers [102–104]. MOF-enzyme composites are also excellent catalysts for the degradation of organic pollutants.

MOF-enzyme composites show better catalytic activity, stability and reusability due to the protection of natural enzymes by MOFs [105]. Multifunctional groups on the surface of MOFs can contribute to improving the activity of immobilized enzymes. Furthermore, MOF nodes and linkers could offer numerous anchor sites for enzymes through chemical bonding, including coordinative bonding, covalent bonding and van der Waals forces [106, 107], which could prevent enzyme denaturation when exposed to extreme conditions and organic solvents. Liu et al. reported a hierarchically porous (HP) MOF HP-PCN-224(Fe) for glucose oxidase (GOx) immobilization [108]. Compared with free GOx, GOx@HP-PCN-224(Fe) displayed higher activity, pH and thermal stability. Park et al. found that *Candida antarctica* lipase B (CAL-B) conjugated on isoreticular MOF-3 (IRMOF-3) exhibited approximately 1000-fold higher activity than free CAL-B [109]. The immobilized enzyme showed higher thermal stability than the free enzyme and superior storage stability. Li et al. encapsulated organophosphorus acid anhydrase (OPAA) into zirconium MOF PCN-128y for the nerve agent simulant diisopropyl fluorophosphate (DFP) detoxication [110]. After three days of dry storage, OPAA@PCN-128y maintained 90% hydrolysis efficiency, while OPAA had only 30% hydrolysis efficiency. They further researched the catalytic performance of OPAA@PCN-128y for the real nerve agent, Soman, which indicated that the efficiency of OPAA@PCN-128y reached 90% in 60 min.

MOF-enzyme composites can remove organic pollutants through both the degradation activity of the encapsulated enzymes and the adsorption capacity of MOFs. Wang et al. found that encapsulation in Cu-MOF (HKUST-1) could enhance the catalytic activity of laccase [111] (Fig. 4a). The laccase/MOF system showed 50% higher degradation efficiency for bisphenol A (BPA) than free laccase. Jiang et al. synthesized the MIL-88A MOF and then used it to immobilize His-tagged organophosphohydrolase (OpdA) for degradation of organophosphorus pesticides (Ops) [112] (Fig. 4c-d). They used OpdA@MIL-88A for the degradation of OPs on grapes and cucumbers, which could achieve almost 100% removal efficiency and retain more than 66% and 61% of initial activity after 6 reuse cycles. Mo et al. encapsulated horseradish peroxidase (HRP) in the single-crystal ordered macroporous zeolitic imidazolate framework-8 (SOM-ZIF-8), which accelerated the degradation process of hazardous dyes (Fig. 4b) [113]. The HRP@SOM-ZIF-8 could rapidly remove congo red (CR) and rhodamine B (RB) by integrating the benefits of oxidative degradation by HRP with adsorption to the host material, exhibiting high removal efficiencies within 2 min. Wang et al. encapsulated the organophosphorus hydrolase (OPH) into Zn-doped Co-based ZIF (0.8CoZIF) for the effective detoxification of methyl parathion (MP) [114]. In the presence of 50 mM $NaBH_4$, the OPH@0.8CoZIF completely converted 95 μM MP and produced nearly 100% 4-aminophenol within 15 min.

### 3.3 MOF nanozyme-catalyzed degradation

By modulating the metal ion nodes and organic ligand, MOFs can be endowed with enzyme-like activities, including oxidase-, peroxidase-, and alkaline phosphatase-like activity, which can contribute to the removal of organic pollutants [115]. MOF-based nanozymes with oxidase-like activity can activate $O_2$ to produce reactive oxygen species (ROS), which in turn can directly oxidize the pollutants [100]. In peroxidase-mimicking MOF nanozymes, MOFs can catalyze the reaction of $H_2O_2$ with

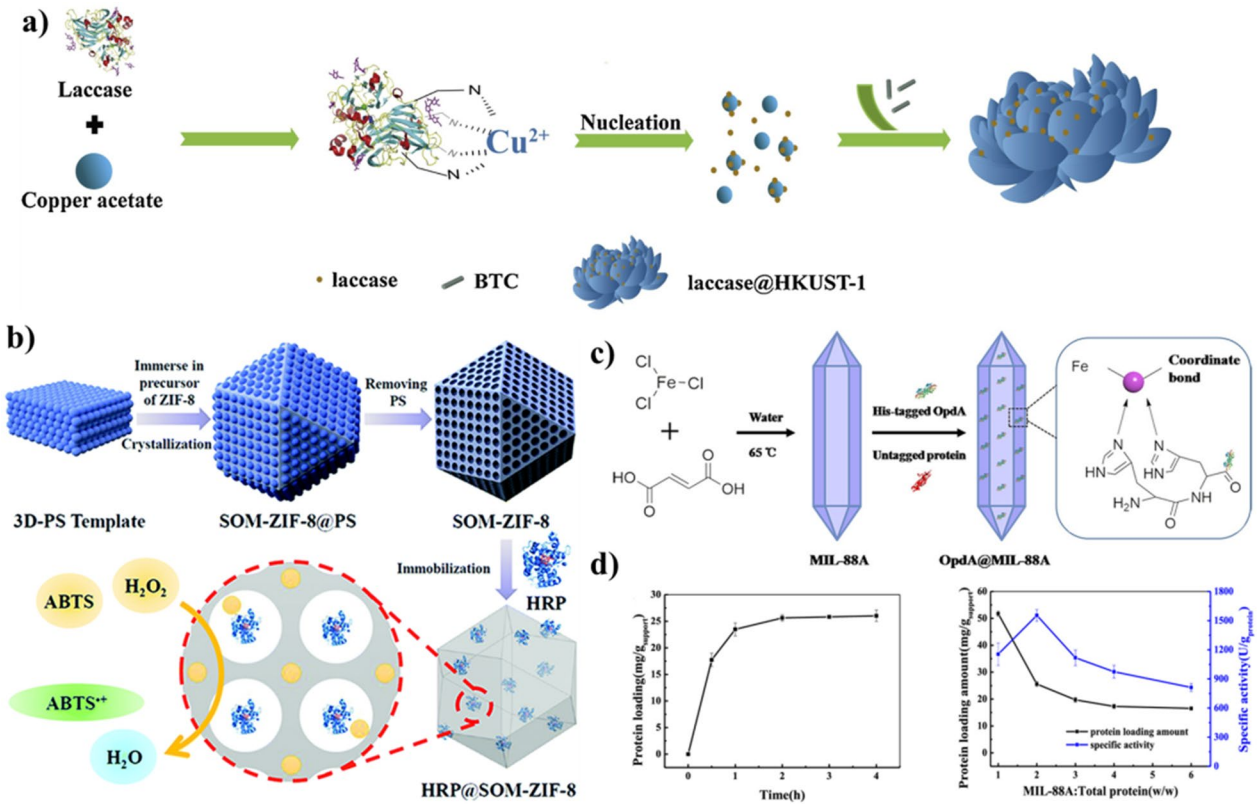


**Fig. 4** **a** Schematic illustration of the synthesis of laccase@HKUST-1 [111] (with kind permission from Elsevier) **b** Schematic diagram of the preparation of HRP embedded in SOM-ZIF-8 [113]. **c** Preparation of MIL-88A and OpdA@MIL-88A [112] (with kind permission from American Chemical Society) **d** Effect of adsorption time on the loading amount of His-OpdA at a 2:1 ratio (w/w) of MIL-88A to total protein; protein loading and activity of immobilized His-tagged OpdA at different ratios (w/w) of MIL-88A to total protein [112] (with kind permission from American Chemical Society)

other substrates [116]. For example, Zhou et al. reported PCN-222(Fe) containing Fe-TCPP as a heme-like ligand, mimicking the heme ligand of peroxidases [117]. In addition, MOFs can be used as hydrolase mimics which catalyze the hydrolysis of chemical bonds to achieve pollutants removal [100, 116]. Compared to natural enzymes, the MOF-based nanozymes show improved catalytic activity, better storage stability, and lower cost.

Luo et al. used three MOFs (MIL-100, MIL-53 and MIL-68) with peroxidase-like activity for aflatoxin B1 (AFB1) removal (Fig. 5a-b) [12]. The removal efficiency reached up to 100%, and animal feeding experiments confirmed that the hepatotoxicity of AFB1 can be neutralized by these peroxidase-like MOFs. Huang et al. reported hollow bimetallic Co-based nanocages (HNCs) (C-CoM-HNC, M = Ni, Mn, Cu, and Zn) for rhodamine B (RhB) degradation (Fig. 5c) [118]. In the strategy, the incorporation of secondary metal ions (Ni, Mn, Cu, and Zn) could provide new active sites and form synergistic active sites with Co. Meanwhile, C-CoM-HNC could mimic the oxidase enzyme and activate PMS, resulting in highly efficient RhB degradation. The C-CoCu-HNC had better oxidase activity than other HNCs and exhibited a promising catalytic performance. Therefore, C-CoCu-HNC was used for RhB degradation and the degradation efficiency could reach 93.41% after 60 min of reaction. They also reported peroxidase-mimicking $NH_2$-MIL-88B(Fe) used for methylene blue (MB) degradation in water [119]. $NH_2$-MIL-88B(Fe) could achieve 90% MB removal efficiency.

In addition, the current peroxide degradation systems are mainly based on the addition of $H_2O_2$ as a peroxidation agent. Zhao et al. developed an Au–Au/$IrO_2$@Cu(*p*-aminobenzoic acid, PABA) catalytic reactor with tandem enzyme-like activity [120], which can exhibit excellent GOx- and peroxidase-like activity (Fig. 5d). More importantly, based on its GOx-like activity, the reactor can convert glucose into $H_2O_2$, which in turn can be used for the oxidation of organic dyes, avoiding the need to handle concentrated $H_2O_2$ with strong oxidizing and corrosive properties. In situ $H_2O_2$ generation therefore provides a

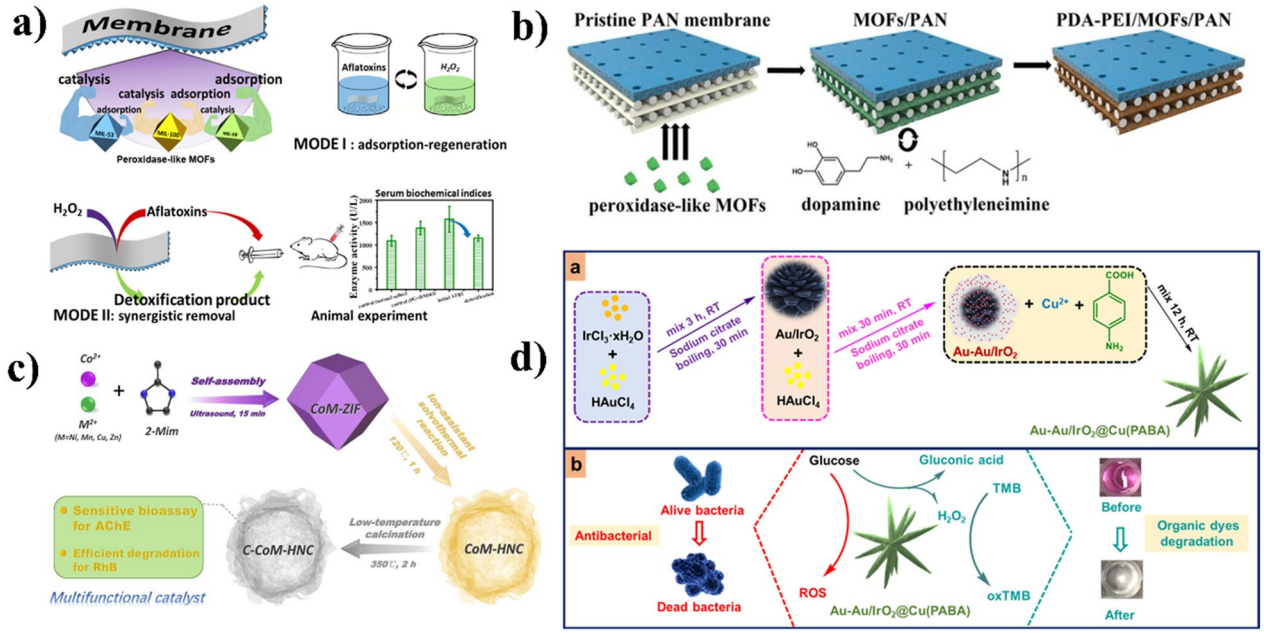


**Fig. 5** **a** MOF-loaded membranes for AFB1 removal [12] (with kind permission from American Chemical Society) **b** Schematic diagram of membrane preparation [12]. **c** Illustration of a general approach for C-CoM-HNC synthesis [118] (with kind permission from American Chemical Society) **d** Schematic illustration of the sensing platform for organic dye degradation with antibacterial activity based on the Au–Au/$IrO_2$@Cu(PABA) cascade reactor [120] (with kind permission from American Chemical Society)

promising direction for the development of novel MOF-based nanozymes.

Most studies focused on the oxidase- or peroxidase-like activity of MOF-based nanozymes. At present, there is little research on MOF nanozymes with hydrolase activity. However, Lin et al. reported a ZIF-90 nanozyme with organophosphate hydrolase (OPH) activity for the hydrolysis of MP (Fig. 6) [121]. The experimental results indicated that the mechanism for MP hydrolysis by ZIF-90 nanozyme could be ascribed to the synergistic effect of zinc and imidazole.

### 3.4 Photocatalytic degradation

As a green degradation technology based on solar energy, photocatalysis holds great promise for the degradation of pollutants [122, 123] (Table 2). To date, numerous photocatalysts have been used for the degradation of organic pollutants, including g-$C_3N_4$, $TiO_2$, ZnO, CdS and their derivatives [124, 125]. Dionysiou et al. reported the use of nitrogen- and fluorine-doped titanium dioxide (NF-$TiO_2$) for microcystin-LR (MC-LR) degradation [126]. Gong et al. found that g-$C_3N_4$/pyromellitic diimide (PDI)-g-$C_3N_4$ homojunction could photocatalytically degrade atrazine (ATZ) [127]. However, there are shortcomings in these photocatalysts, such as limited visible light utilization, improper band position and rapid recombination of charge carriers, which lead to low photocatalytic efficiency [128]. As porous coordination polymers consisting of tunable metal clusters and organic linkers, MOFs have photochemical properties. Considering the rich variety of possible MOF structures, using narrow gap semiconductors to construct MOF-based composites could overcome the above drawbacks and inherit the advantages of the individual MOFs or semiconductors [129–131]. For example, in order to make up for shortcomings such as the wide band gaps, insufficient light response and insufficient electric charge transfer rate, researchers introduced porous metal oxides, carbon materials, metal sulfides (MSs) and their heterostructures to form composites with improved photocatalytic performance [132, 133]. In an effort to even better support practical applications of MOFs in photocatalysts, the relevant theoretical calculation of MOF catalyst was elaborated by Hai and his colleague [134], guides the design and development of MOFs material. Kim et al. reported a novel MIL-125(Ti) modified with chemically reduced nitrogen-containing graphene oxide (CR–N-GO), named r-N-MIL [135]. With the incorporation of CR–N-GO, the pore size was increased from 2 nm to 2.8 nm, and the band gap of the semiconductor material was narrowed, which finally improved the photocatalytic activity of r-N-MIL. Wang et al. fabricated sulfur (S)-$TiO_2$/UiO-66-$NH_2$ to achieve $Cr^{6+}$ reduction and BPA oxidation [136]. Wang et al. reported a $ZnIn_2S_4$@PCN-224 heterojunction that could degrade 99.9% tetracycline hydrochloride (TCH) within 60 min (Fig. 7) [137]. The increased photocatalytic

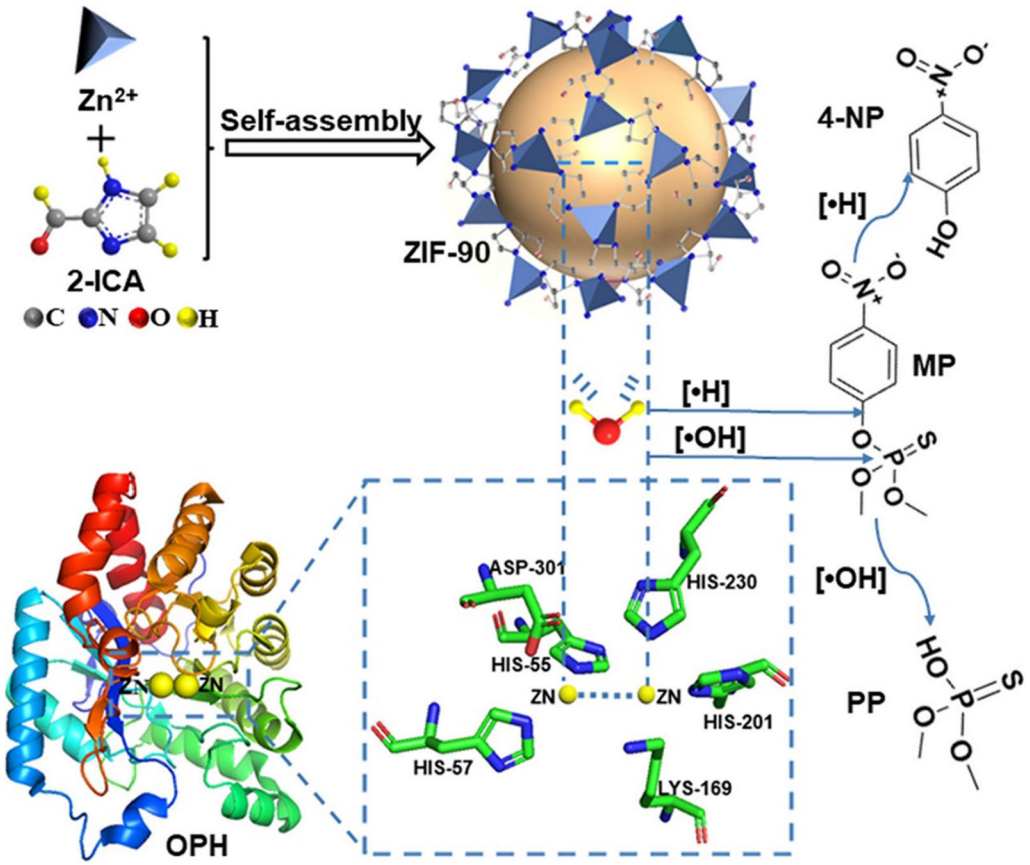


**Fig. 6** Schematic representation of the synthesis of ZIF-90 and the reaction mechanism of organophosphorus hydrolase and ZIF-90 [121] (with kind permission from American Chemical Society)

performance of $ZnIn_2S_4$@PCN-224 compared to pure $ZnIn_2S_4$ was attributed to the construction of a hierarchical heterostructure between $ZnIn_2S_4$ and PCN-224.

The construction of heterojunctions is an ideal strategy for improving the photocatalytic efficiency of MOFs, which can inhibit the rapid recombination of

**Table 2** Summary of the photocatalytic degradation performance of functionalized MOFs as catalysts for the removal of organic pollutants

| Pollutant | MOF | Pollutant concentration | Time (min) | Degradation efficiency (%) | Refs |
|---|---|---|---|---|---|
| Styrene | $TiO_2$@$NH_2$-UiO-66 | 30 ± 1 ppm | 600 | 99 | [138] |
| Acetaldehyde | GO/$NH_2$-MIL-125(Ti) | 5.0 μL | 80 | 65 | [139] |
| RhB | PCN/MIL | 10 mg $L^{-1}$ | 200 | 86.9 | [140] |
| MB | UiO-66/g-$C_3N_4$ | 10 mg $L^{-1}$ | 240 | 100 | [141] |
| RhB | $[(Cu_4Cl)(CPT)_4]\cdot(HSiW_{12}O_{40})\cdot 31H_2O$ | 10 ppm | 80 | 99 | [142] |
| Cr(VI) | $NH_2$-MIL-68 (In0.4Fe0.6) | 20 mg $L^{-1}$ | 120 | 99.29 | [143] |
| TC-HCl | $NH_2$-MIL-68 (In0.4Fe0.6) | 20 mg $L^{-1}$ | 120 | 71.53 | [143] |
| RhB | $TiO_2$ NPs/PCN-222(Zn) | 50 mg $L^{-1}$ | 270 | 100 | [144] |
| 2,4-DNP | $TiO_2$ NPs/PCN-222(Zn) | 20 mg $L^{-1}$ | 270 | 68 | [144] |
| Diclofenac (DF) | PCN-134 | 0.1 mM | 300 | 99 | [145] |
| Phenol | Pt@UiO-66-$NH_2$ thin film reactor | $3.5\times10^{-5}$ M | 300 | 70 | [146] |

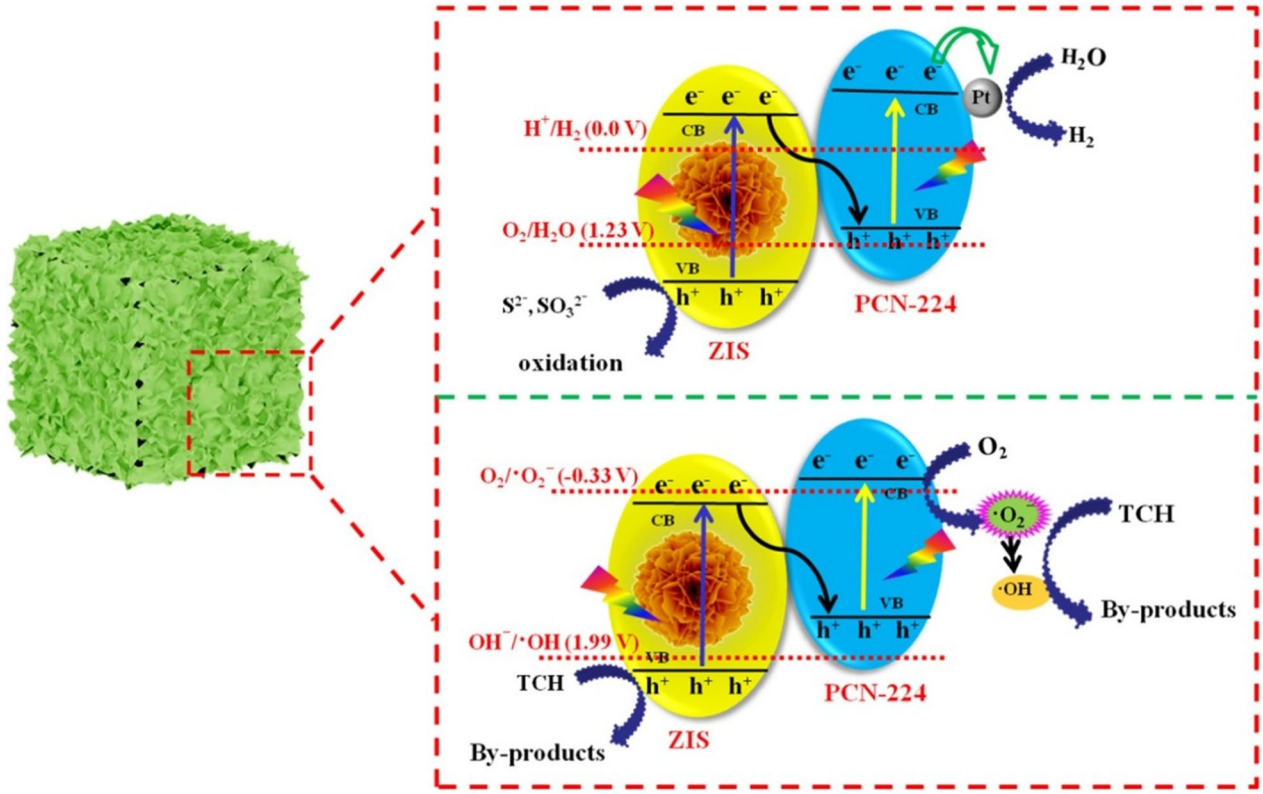


**Fig. 7** The mechanism of the electron/hole transfer and separation process of the ZIS@P20 composite under visible light irradiation [137] (with kind permission from Wiley–VCH)

photogenerated electrons and holes [147]. In recent years, type II composite heterojunctions combining MOFs with $TiO_2$ have exhibited superior photocatalytic efficiency compared with pure MOFs or $TiO_2$ [137]. Zhao et al. reported the photocatalyst PCN-222(Mn)-$PW_{12}$/$TiO_2$, which degraded 94.83% for ofloxacin in 120 min and 98.5% for RhB in 80 min [148]. The $N_2$ adsorption–desorption and photoluminescence (PL) spectra indicated that the introduction of PCN-222(Mn) increased the number of active sites in PCN-222(Mn)-$PW_{12}$/$TiO_2$. The recombination rate of photoinduced electron–hole pairs was reduced, which in turn improved the photocatalytic efficiency. Liu et al. prepared 2D/1D core–shell heterostructures ($ZnIn_2S_4$@$Fe_3O_4$ and $ZnIn_2S_4$@α-$Fe_2O_3$) [149], and characterized them through a series of electrochemical measurements, including transient photocurrent responses, EIS Nyquist plots and polarization curves. The results showed that the 2D/1D core–shell heterostructures were beneficial for electron transfer, which facilitated the photodegradation of RhB. Lu et al. used g-$C_3N_4$/PDI@MOF heterojunctions as photocatalysts for the removal of TC, carbamazepine (CBZ), BPA and p-nitrophenol (PNP) [150].

As an emerging and effective method, these studies demonstrated the potential of functionalized MOFs in photocatalytic degradation for the removal of organic pollutants. Nevertheless, the research on MOF-based degradation of organic pollutants is still in its infancy. This research area remains challenging due to the complex reaction environments, such as photocatalytic reactors required for these catalysts and the relatively low degradation efficiency obtained. Moreover, it is a promising strategy for constructing MOF-based photocatalysts to remove pollutants and develop novel photocatalysts with high-efficiency optical and electronic properties. In addition, photocatalysis can also be combined with other reactions, including Fenton and SR-AOPs, which may increase the degradation efficiency.

### 3.5 MOF catalyst performance in the Fenton-like process

In Fenton and Fenton-like reactions, ferrous ion ($Fe^{II}$) acts as a catalyst on $H_2O_2$ to produce •OH, which in turn can attack even recalcitrant organic pollutants [151, 152]. However, conventional homogenous Fenton and Fenton-like reactions have various disadvantages, such as secondary pollution and the need for pH regulation [153,

154]. To avoid these disadvantages, the superior heterogeneous Fenton-like reactions, including photo-Fenton reaction, Hetero-electro-Fenton process and photo-electro-Fenton (PEF) reaction, have stood out.

Iron-based MOFs (Fe-MOFs) are a class of good photocatalysts and can be more efficiently coupled with Fenton reagents than other MOFs. Mei et al. reported benzimidazole (BIm)-modified Fe-MOFs, and the rod-like α-$Fe_2O_3$-x exhibited complete MB degradation [155]. The oxygen vacancies (OVs) and $Fe^{2+}$ content determined the α-$Fe_2O_3$-$_x$ photo-Fenton-like catalytic activity, which was substantiated by the experimental data and density functional theory (DFT) calculations. Wang et al. reported a UiO-66-based MOF conjugated with an FeIII metalloporphyrin that could integrate photocatalysis and Fenton-like processes to degrade RhB [156] (Fig. 8a). Fe(III) tetra(4-carboxylphenyl)porphyrin chloride (FeIII-TCPPCl) not only played the role of a photosensitizer, but also acted as an iron-based catalyst that produced ·OH from $H_2O_2$, which could accelerate the Fenton-like process. Liu et al. used MIL-88A as a catalyst for the degradation of tris-(2-chloroisopropyl) phosphate (TCPP), a widely used organophosphorus flame retardant with adverse effects on the nervous system [157] (Fig. 8b). In the MIL-88A/$H_2O_2$/Vis system, the degradation efficiency of TCPP reached approximately 95% (Fig. 8c). These were ascribed to the Fe–O clusters in MIL-88A, which could activate $H_2O_2$ and then form ·OH radicals. Owing to the slow Fe(II)/Fe(III) cycle, the efficiency of Fenton and Fenton-like reactions is generally limited. Huang and co-workers reported a two-dimensional (2D) π-d conjugated MOF named $Fe_3(HITP)_2$ (HITP = 2,3,6,7,10,11-hexaiminotriphenylene) with high conductivity, which accelerated the Fe(III)/Fe(II) cycle to achieve 96.7% TC degradation within 30 min [158]. Furthermore, the efficiency of Fenton-like processes can be enhanced by introducing heterogeneous electro-Fenton catalysts. Electro-Fenton reactions realized catalytic degradation rely on in-situ generation of $H_2O_2$ on the cathode by $O_2$ reduction and further conversion to ·OH

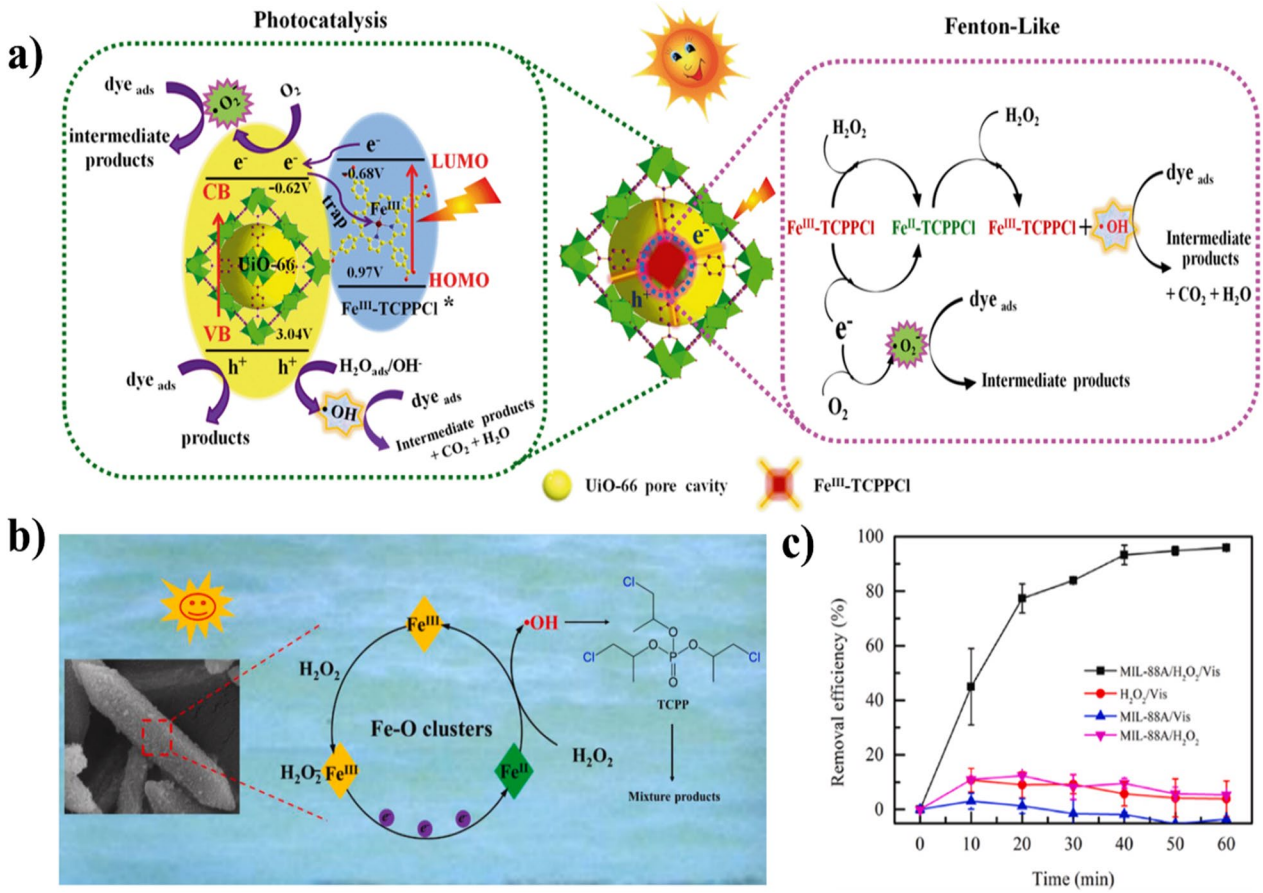


**Fig. 8** **a** The proposed photocatalytic mechanism of FeIII-TCPPCl ⊂ UiO-66 in the co-catalytic Fenton-like reaction [160] (with kind permission from Elsevier) **b** Schematic diagram of the reaction mechanism of the MIL-88A/$H_2O_2$/Vis system [161] (with kind permission from Elsevier) **c** The efficiency of different systems in the removal of TCPP [161]

[159]. Wu et al. have achieved electro-Fenton degradation of SMX through the use of $Mn_{0.67}Fe_{0.33}$-MOF-74. The SMX removal efficiency can reach 96% at pH 3 and 30 mA of current after 90 min [160]. Huang's team prepared a series of $Mn_xCo_{3-x}$@C-GF with excellent catalytic performance by introducing Mn/Co MOFs derivatives into the graphite felt cathodes [161]. In their work, the CIP removal efficiency could achieve 99.8% in 60 min, which could be attributed to the electrochemically active metals that promoted the generation of active radicals (·OH). Another example of heterogeneous Fenton-like processes is the PEF reaction, which is an upgraded EF process. Ye and his colleagues [162] used 2,2′-bipyridine-5,5′-dicarboxylate (bpydc) as a linker to prepare heterogeneous PEF catalyst Fe − bpydc 2D MOF for bezafibrate treatment. Under UVA and visible light irradiation, bezafibrate in solution could be removed completely with a small amount (0.05 g $L^{-1}$) Fe − bpydc 2D MOF as a catalyst. The experimental analysis and theoretical calculations revealed that newly developed MOFs have become highly efficient Fenton-like catalysts [163, 164].

### 3.6 MOF catalytic degradation performance in SR-AOPs

SR-AOPs produce hydroxyl radicals (·OH) and sulfate radicals ($SO_4^{\bullet-}$), which give them great potential for efficiently eliminating a variety of harmful pollutants. In SR-AOPs, $SO_4^{\bullet-}$ and singlet oxygen ($^1O_2$) are mainly produced, which contribute to the activation of persulfate (PS) and peroxymonosulfate (PMS) [155]. Electron paramagnetic resonance (EPR) analyses, and theoretical calculations based on DFT are used to explore the possible mechanisms in MOFs-based SR-AOPs [165], which demonstrated that PMS/PDS activation by MOFs-based materials for organic pollutants degradation is promising. PDS and PMS were activated by many strategies, including ultraviolet irradiation, chemical methods and other methods in which photo-activation deserves special attention [166]. In addition, partially coordinated metal ions in MOFs can activate PMS/PS to form $SO_4^{\bullet-}$ and ·OH, and thus degrade organic pollutants. Liu et al. embedded Co sites in a carbon nitride catalyst (CoCN), which were used for visible light-induced PMS activation [167]. The results of the radical quenching experiments and EPR analyses indicated the reaction mechanism of BPA degradation. The rate constant for the CoCN/Vis/PMS system (1.84 $min^{-1}$) was 5.58 times higher than that of the CoCN/ PMS system (0.329 $min^{-1}$), which indicated that visible light could help improve the activation performance of CoCN for PMS and produce more reactive free radicals to degrade BPA.

In addition, bimetallic MOFs exhibited several synergistic effects and enhanced properties compared with the monometallic MOFs. Roy et al. reported bimetallic MOF-based heterojunction MIL-53(Fe/Co)/$CeO_2$ for atrazine degradation [168]. Visible light irradiation only achieved 24.3% ATZ degradation within 60 min, while the MIL-53(Fe/Co)/$CeO_2$/PMS/Vis system could achieve 99.9% ATZ degradation. The results indicated that the Co and Fe sites in MIL-53(Fe/Co) could achieve simultaneous redox cycles and consequently activate PMS and generate the reactive species.

The above studies indicated that increasing metal sites could greatly improve PMS activation performance. This phenomenon can also be reflected in PS activation, which is based on MOFs. For example, Duan et al. fabricated Cu-MIL-101(Fe) andCo-MIL-101(Fe) to degrade Acid Orange 7 (AO7) via PS activation [169]. Compared with pristine MIL-101(Fe), the AO7 removal efficiency by 6 wt% Cu-MIL-101(Fe) and 6 wt% Co-MIL-101(Fe) has reached 92% and 98% within 150 min.

The SR-AOPs are still in their infancy, and more research is needed to understand their complex catalytic mechanisms.

### 3.7 Other MOF-based catalytic degradation

In addition to the above catalytic reactions, electrochemical catalytic degradation and ultrasonic reactions are important processes in the removal of pollutants. MOF-based materials are widely used as electrode active materials in the electrocatalytic degradation of organic pollutants. Arulpriya et al. [170] synthesized a MOF-modified electrode by introducing $TiO_2$@Fe MOF for the simultaneous sensing and degradation of CPF. The $TiO_2$@Fe MOF/SPE could degrade the chlorpyrifos with high efficiency due to its electrocatalytic activity. Xu et al. [171] introduced UiO-66 derived $ZrO_2$-C nanoparticles into $PbO_2$ electrode to construct a new type of $ZrO_2$-C/$PbO_2$ anode. The prepared functional electrode possessed advantageous electrochemical performance with the 2, 4, 6-trinitrophenol (TNP) removal efficiency of up to 94.48% in 140 min. In addition, MOF-derived nanomaterials can also be introduced into the electrode as photoelectrodes to enhance light utilization and improve degradation efficiency [172]. Jia et al. [173] used ZIF-8/NF-$TiO_2$ nanocomposites as photoanodes for the degradation of sulfa antibiotics. Results showed that the hybrid photoelectrode can effectively improve light utilization and enhance electron–hole pairs, resulting in enhanced the photo-electrocatalytic degradation activity.

With respect to the ultrasound (US) process, coupled with photocatalysis, it could improve the degradation efficiency of organic compounds [174]. Mosleh et al. [175] prepared a novel photocatalyst by doping the Ce and Eu with HKUST-1 MOF for treating

organophosphorus pesticide Malathion by sonophotocatalysis. More cavitation bubbles were generated and climaxed the mass transfer rate due to the ultrasonic field, resulting in a significantly improved Malathion degradation rate. Moreover, the sonolysis process has been presented for PS activation, which showed enhanced effects on the degradation of organic pollutants [176]. In Sajjadi and colleagues' work, $Fe_3O_4$@MOF-2 was prepared as a heterogeneous nanocatalyst for PS activation under US irradiation to degrade diazinon [176]. In the presence of US irradiation, the $Fe_3O_4$@MOF-2/US/PS process accomplished the degradation of diazinon completely in 60 min, which could be attributed to the intensified generation of hydroxyl radicals by US. The hybrid systems integrating ultrasound and various AOPs are a low-cost and effective technique for organic contaminants treatment [177].

### 3.8 Reusability and safety of MOF catalysts

In practical applications, MOF catalysts are difficult to separate from the reaction solution for recycling. The fragile powder form of MOFs caused poor processing and recycling properties, which limit their practical applications [178, 179]. However, numerous strategies have been developed to overcome these defects. One is synthesizing magnetic MOF compounds. Niu et al. reported a CuCo/C catalyst which could degrade 90% CIP by activating PMS within 30 min [180]. The hysteresis curve revealed that CuCo/C could be easily separated using an external magnetic field (Fig. 9a). Cong et al. reported a yolk-shell $Fe_3O_4$@MOF-5 nanocomposite for MB removal [181]. In the yolk-shell $Fe_3O_4$@MOF-5, $Fe_3O_4$ was magnetic and catalytic, while the MOF-5 shell could effectively protect the $Fe_3O_4$ while providing numerous pores to accelerate the molecular

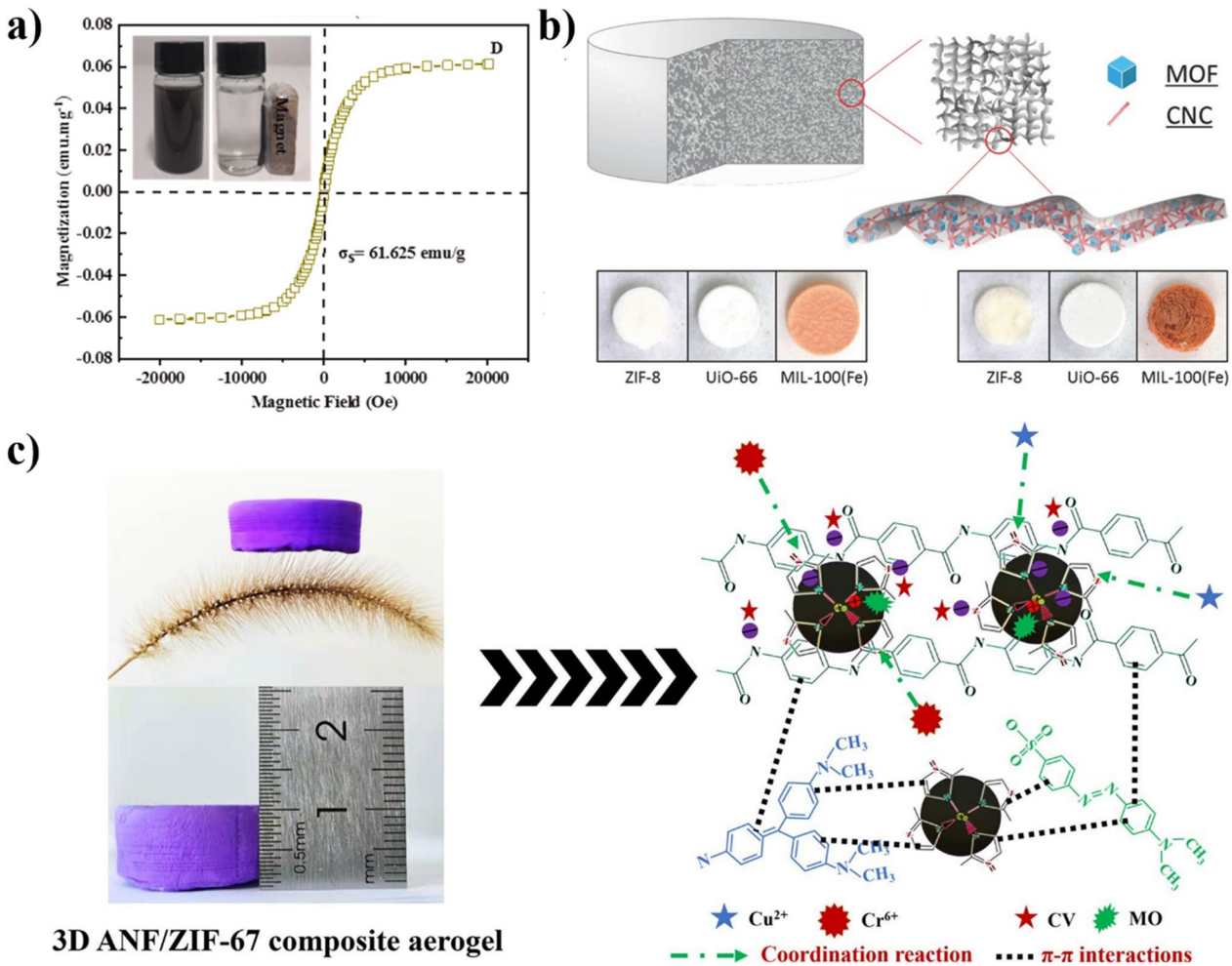


**Fig. 9** **a** Time-dependent adsorption (correlation curve was drawn using the kinetic parameters calculated from the pseudo-second-order model), pseudo-second-order plots (inset) and photographs of the contaminated aqueous solution before and after adsorption of RhB on MIL-100(Fe) (33.3wt.%) aerogel [182] (with kind permission from Wiley–VCH) **b** Magnetic properties of CuCo/C [180] (with kind permission from Elsevier) **c** Scheme of π-π and electrostatic interactions between the 3D ANF/ZIF-67 composite aerogel and dyes [183] (with kind permission from Elsevier)

transfer and improve the catalytic efficiency. Due to the $Fe_3O_4$ yolk, $Fe_3O_4$@MOF-5 could also be separated using an external magnetic field.

Another effective recycling strategy is fixing MOFs on suitable carriers such as membranes or hydrogels/aerogels (Fig. 9b). Wang et al. used zeolitic imidazolate framework (ZIF)-67/PAN(polyacrylonitrile) composite nanofibers to activate PMS in the catalytic degradation of acid yellow-17 (AY) [184]. Different from dispersed MOF nanoparticle materials, the ZIF-67/PAN composite nanofibers could be easily separated from the reaction system due to their flexibility. He et al. reported Co@NCNT-MS catalysts with a favorable TC degradation capacity [185]. Researchers encapsulated the catalysts in graphene oxide (GO) by facile vacuum filtration to form a composite membrane with outstanding ease of separation. He et al. constructed a ZIF-8 photocatalyst membrane and its derived product (ZnS photocatalyst membrane) for the removal of MB under visible light irradiation [186]. The ZIF-8 photocatalyst membrane could easily achieve complete separation and avoid secondary contamination. Yao et al. reported hybrid aerogels made from ZIF-9 and ZIF-12 loaded onto cellulose aerogels [187]. The hybrid aerogels could remove about 90% of PNP in 60 min and could also be easily removed from the reaction system. Zhao et al. prepared a 3D aramid nanofiber (ANF)/ZIF-67 composite aerogel for the removal of organic dyes [183]. The 3D ANF aerogel served as a mechanical support to achieve the uniform assembly of ZIF-67 (Fig. 9c). Ren et al. designed and synthesized the MOF composite material copper-benzenedicarboxylate/cellulose aerogel (CuBDC/CA) [188], which could decompose more than 90% methylene blue in 240 min.

### 3.9 Functional MOF-based derivative for catalytic degradation

To achieve the superior performance of catalytic, pristine MOFs and MOF composites can be converted into derivatives by direct pyrolysis under appropriate conditions. MOF derivatives, synthesized via different pyrolysis strategies, are promising catalysts and absorbents for various reactions. For example, nanoporous metal-containing carbon (metal@C) catalysts are manufactured from MOFs via pyrolysis under an inert atmosphere (nitrogen or argon). Li and colleagues successfully synthesized a core/shell structured hollow Fe–Pd@C nanomaterial by carbonizing Fe-metal organic frameworks in the $N_2$ atmosphere [189]. The as-synthesized nanomaterials show excellent performance as catalysts in strengthening homogeneous Fenton degradation of phenol. Moreover, porous regular-shaped metal oxide@C can be obtained when the MOFs are calcinated in reactive environments such as an oxygen atmosphere. Zhang and coworkers [190] constructed MOF-derived $ZnFe_2O_4/Fe_2O_3$ perforated nanotubes as catalysts for ciprofloxacin (CIP) photocatalytic removal. In their work, the magnetically recoverable Z-scheme photocatalysts were successfully synthesized by one-step calcination method using MOF as a precursor. Under light irradiation, with the help of the prominent photocatalytic performance of $ZnFe_2O_4/Fe_2O_3$ perforated nanotubes, the CIP removal percentage increased to 96.5% within 180 min.

In addition, the development of heterogeneous SR-AOPs based on MOF composites and their derivatives has drawn much attention. Pu et al. reported a MOF-derived novel magnetic Fe@C composite for PS activation and SMX degradation [191]. Fe@C-800, synthesized under the pyrolysis temperature of 800 °C, exhibits high catalytic capacities. Degradation efficiency for SMX is 98.3% and decomposition magnitude for PS is 93.6% after 90 min. Zhao and coworkers reported the $CeO_2$/N-doped carbon/Ce-TCPP heterostructures that were converted from Ce-TCPP by performing a simple pyrolysis process at low temperature under $N_2$ flow [192]. The prepared heterostructures as heterogeneous catalyst exhibit excellent photocatalytic activity of PMS under visible light, with the degradation rates of 98.6% and 94.4% for MB and MO within 60 min, respectively. The above works provided a possible degradation strategy for remediation of organic pollutants from the leather production.

### 3.10 MOF-functionalized products for pollutant removal

MOFs hold great promise as novel materials for the removal of pollutants, and integrating them into functionalized materials is very important from a practical point of view. Agrawal et al. fabricated MOF-functionalized fabrics ZIF-8@ carboxymethylated (CM) cotton and ZIF-67@CM cotton for the removal of volatile organic compounds (VOCs) from ambient air (Fig. 10) [193]. These fabrics have enormous potential for application in protective textiles, anti-odor clothing, air purification filters, and related products. Yoo et al. coated cotton with Zr-MOFs such as UiO-66, UiO-67 and DUT-52 and utilized the resulting composite for the removal of particulate matter PM from air, which could improve the performance of air filters [194]. Tahazadeh et al. synthesized biodegradable cellulose acetate/MOF-derived porous carbon (CA/MOFDPC) adsorptive membranes for MB removal [195]. These functionalized products have a number of potential commercial applications. Seo et al. prepared nanocellulose/MOF aerogel composites for effective detoxification of methyl paraoxon (MPO) in both static and dynamic continuous flow systems [196].

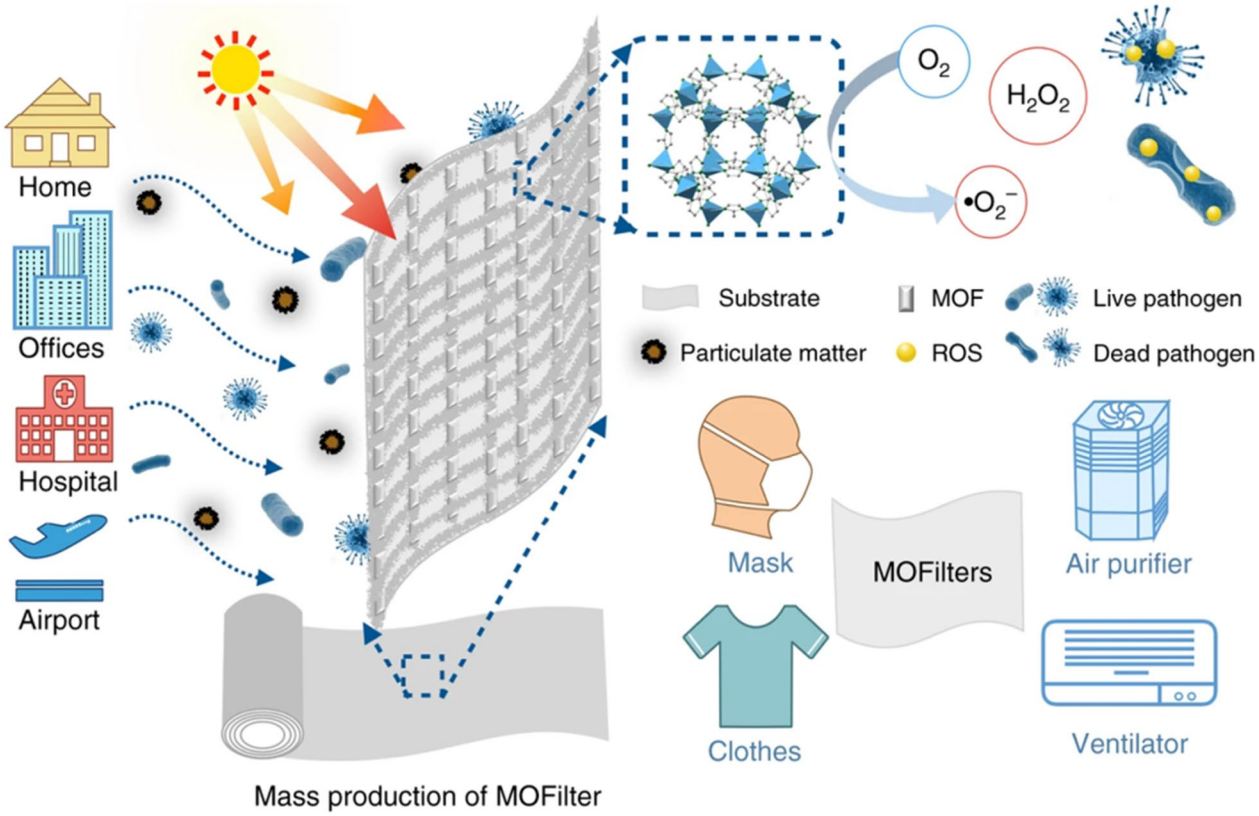


**Fig. 10** Schematic representation of MOF-based filters for integrated air purification [193] (with kind permission from Elsevier)

## 4 Conclusions and perspectives

In this article, we reviewed recent progress in treatment methods for removing organic pollutants, with a focus on catalytic degradation using MOFs. First, we described the synthesis methods of MOFs. Although solvothermal synthesis is the most popular strategy for the preparation of MOFs, other green strategies have been developed to avoid high energy consumption or the residue generation, which will gradually become the direction of the future. Then, recent advances in the applications of MOFs in the catalytic degradation of organic pollutants were systematically reviewed. MOF nanozymes have been found to have wide applications in pollutant removal due to their multiple enzyme-like activities, but they still face the challenge of further hoisting their stability in practical applications. The photocatalytic processes based on MOFs can degrade organic pollutants effectively in a sustainable way through the use of solar energy as energy sources. The heterogeneous Fenton-like reaction using solid catalysts removes organic contaminants by producing reactive species on the surface of the catalysts in an environmentally benign way. Meanwhile, research in this field is still in the early stages and some disadvantages, including aggregation and dispersibility, still exist. MOF-based materials exhibited high activity in the SR-AOPs process for the removal of organic pollutants due to their unique structural characteristics, and the catalytic performance in the field of SR-AOPs is often limited by activation time and temperature. Notably, MOFs can be combined with other nano- and functional materials to achieve synergistic effects. Currently, MOFs are gradually being developed from enzyme carriers and physical adsorbents into multifunctional materials with enzyme-mimetic catalytic activity and photocatalytic properties. With the progress of synthesis methods, multi-site transformation can be achieved, while the adsorption performance, enzyme catalysis, photocatalysis performance, and even auxiliary detection and removal functions can be achieved, resulting in truly multifunctional materials for the future. Finally, the heterogeneity of MOFs and their combination with hydrogels, aerogels or membranes will enable facile separation and recovery, which is very important for practical applications. We hope this review can provide useful information for researchers, and provide a reference for the removal of organic pollutants with MOF in the leather industry.

Further research on the removal of organic pollutants with MOFs should address the following issues:

1. Although the synthesis methods of most MOFs are simple, the costs remain high. We need to develop more cost-effective methods to fabricate MOFs, such as strategies to choose cheaper organic ligands.
2. Currently, experiments on the removal of pollutants using MOFs remain at the laboratory scale. In actual samples, there are many other substances which could disturb the removal process. Therefore, it is essential to evaluate these removal methods of organic pollutants for practical application.
3. Further studies should include specific experiments on the industrial utilization of MOFs. Although researchers have studied MOF-based catalysts in membrane reactors and MOF-based adsorbents as carriers, there are few studies on the removal of pollutants in large-scale industrial scenarios.

Given the above problems and challenges, researchers could synthesize new types of MOFs materials and optimize the methods to reduce the influence of the material itself on the experimental results, thus solving the problems of materials in practical applications. In summary, MOFs, as an excellent new porous nanomaterial, would be able to achieve large-scale industrial production and practical application in the near future with the joint efforts of researchers.

**Acknowledgements**
We gratefully appreciate the support from The National Key Research and Development Program of China (No, 2020YFC1606801).

**Author contributions**
WJH analyzed and interpreted the data regarding the MOF for the removal of organic pollutants from references. YM, WST and WXH invested the MOF for the removal of organic pollutants and reviewed the whole paper. AN sorted out the table and graph in the whole manuscript. LGP revised the whole manuscript and was a major contributor in revising the manuscript. WLN reviewed and edited the whole manuscript, and was a major contributor in writing the manuscript. All authors read and approved the final manuscript.

**Funding**
This work was supported by the National Key Research and Development Program of China (No. 2020YFC1606801).

**Availability of data and materials**
The datasets generated and/or analyzed during the current study are available in the Web of Science repository.

## Declarations

**Competing interests**
The authors declare that they have no competing interests.

**Author details**
[1]School of Food Science and Pharmaceutical Engineering, Nanjing Normal University, Nanjing 210023, People's Republic of China. [2]Nanjing Customs District Industrial Products Inspection Center, Nanjing 210001, People's Republic of China. [3]National Solid State Fermentation Technology Research Center, Luzhou 646000, People's Republic of China. [4]Institute of Forensic Science, Jiangsu Provincial Public Security Bureau, Nanjing 210024, People's Republic of China.

Received: 5 October 2023 Revised: 27 November 2023 Accepted: 6 December 2023
Published online: 11 December 2023

**References**

1. Morin-Crini N, Lichtfouse E, Fourmentin M, Ribeiro ARL, Noutsopoulos C, Mapelli F, Fenyvesi E, Vieira MGA, Picos-Corrales LA, Moreno-Pirajan JC, Giraldo L, Sohajda T, Huq MM, Soltan J, Torri G, Magureanu M, Bradu C, Crini G. Removal of emerging contaminants from wastewater using advanced treatments A review. Environ Chem Lett. 2022;20:1333–75.
2. Selvasembian R, Gwenzi W, Chaukura N, Mthembu S. Recent advances in the polyurethane-based adsorbents for the decontamination of hazardous wastewater pollutants. J Hazard Mater. 2021;417: 125960.
3. Skorjanc T, Shetty D, Trabolsi A. Pollutant removal with organic macrocycle-based covalent organic polymers and frameworks. Chem. 2021;7:882–918.
4. Wang Y, Chen Y, Jiang L, Huang H. Improvement of the enzymatic detoxification activity towards mycotoxins through structure-based engineering. Biotechnol Adv. 2022;56: 107927.
5. Mondol MMH, Jhung SH. Adsorptive removal of pesticides from water with metal-organic framework-based materials. Chem Eng J. 2021;421:129688.
6. Ran L, Lu B, Qiu H, Zhou G, Jiang J, Hu E, Dai F, Lan G. Erythrocyte membrane-camouflaged nanoworms with on-demand antibiotic release for eradicating biofilms using near-infrared irradiation. Bioact Mater. 2021;6:2956–68.
7. Du CY, Zhang Y, Zhang Z, Zhou L, Yu GL, Wen XF, Chi TY, Wang GL, Su YH, Deng FF, Lv YC, Zhu H. Fe-based metal organic frameworks (Fe-MOFs) for organic pollutants removal via photo-Fenton: a review. Chem Eng J. 2022;431:133932.
8. Dapaah MF, Niu Q, Yu YY, You T, Liu B, Cheng L. Efficient persistent organic pollutant removal in water using MIL-metal-organic framework driven Fenton-like reactions: a critical review. Chem Eng J. 2022;431:134182.
9. Yang F, Du M, Yin K, Qiu Z, Zhao J, Liu C, Zhang G, Gao Y, Pang H. Applications of metal-organic frameworks in water treatment: a Review. Small. 2021;18(11):e2105715.
10. Miloloža M, Cvetnić M, Kučić Grgić D, Ocelić Bulatović V, Ukić Š, Rogošić M, Dionysiou DD, Kušić H, Bolanča T. Biotreatment strategies for the removal of microplastics from freshwater systems. A review. Environ Chem Lett. 2022;20:1377–402.
11. Polman EMN, Gruter GM, Parsons JR, Tietema A. Comparison of the aerobic biodegradation of biopolymers and the corresponding bioplastics: a review. Sci Total Environ. 2021;753: 141953.
12. Ren Z, Luo J, Wan Y. Enzyme-like metal-organic frameworks in polymeric membranes for efficient removal of aflatoxin B1. ACS Appl Mater Interfaces. 2019;11:30542–50.
13. Birhanli E, Noma SAA, Boran F, Ulu A, Yesilada O, Ates B. Design of laccase-metal-organic framework hybrid constructs for biocatalytic removal of textile dyes. Chemosphere. 2022;292: 133382.
14. Du X, Zhou M. Strategies to enhance catalytic performance of metal-organic frameworks in sulfate radical-based advanced oxidation processes for organic pollutants removal. Chem Eng J. 2021;403:126346.
15. Huang DL, Wang GF, Cheng M, Zhang GX, Chen S, Liu Y, Li ZH, Xue WJ, Lei L, Xiao RH. Optimal preparation of catalytic metal-organic framework derivatives and their efficient application in advanced oxidation processes. Chem Eng J. 2021;421:127817.
16. Duan X, Yang S, Wacławek S, Fang G, Xiao R, Dionysiou DD. Limitations and prospects of sulfate-radical based advanced oxidation processes. J Environ Chem Eng. 2020;8:103849.
17. Lin RB, Xiang S, Li B, Cui Y, Qian G, Zhou W, Chen B. Our journey of developing multifunctional metal-organic frameworks. Coord Chem Rev. 2019;384:21–36.

18. Li Z, Li ZJ, Li SJ, Wang K, Ma FB, Tang B. Potential applications of metal-organic frameworks. Coord Chem Rev. 2009;253:3042–66.
19. Katsoulidis AP, Antypov D, Whitehead GFS, Carrington EJ, Adams DJ, Berry NG, Darling GR, Dyer MS, Rosseinsky MJ. Chemical control of structure and guest uptake by a conformationally mobile porous material. Nature. 2019;565:213–7.
20. Freund R, Zaremba O, Dinca M, Arnauts G, Ameloot R, Skorupskii G, Bavykina A, Gascon J, Ejsmont A, Goscianska J, Kalmutzki M, Lachelt U, Ploetz E, Diercks CS, Wuttke S. The current status of MOF and COF applications. Angew Chem-Int Edit. 2021;60:23975–4001.
21. Zhou Z, Mukherjee S, Hou S, Li W, Elsner M, Fischer RA. Porphyrinic MOF film for multifaceted electrochemical sensing. Angew Chem-Int Edit. 2021;60:20551–7.
22. Lin JB, Nguyen TTT, Vaidhyanathan R, Burner J, Taylor JM, Durekova H, Akhtar F, Mah RK, Ghaffari-Nik O, Marx S, Fylstra N, Iremonger SS, Dawson KW, Sarkar P, Hovington P, Rajendran A, Woo TK, Shimizu GKH. A scalable metal-organic framework as a durable physisorbent for carbon dioxide capture. Science. 2022;374:abi7281.
23. Vilela SMF, et al. 2021 Multifunctionality in an ion-exchanged porous metal-organic framework. J Am Chem Soc. 2021;143:1365–76.
24. Haddad S, Lazaro IA, Fantham M, Mishra A, Silvestre-Albero J, Osterrieth JWM, Schierle GSK, Kaminski CF, Forgan RS, Fairen-Jimenez D. Design of a functionalized metal-organic framework system for enhanced targeted delivery to mitochondria. J Am Chem Soc. 2020;142:6661–74.
25. Gao Y, Liu G, Gao M, Huang X, Xu D. Recent advances and applications of magnetic metal-organic frameworks in adsorption and enrichment removal of food and environmental pollutants. Crit Rev Anal Chem. 2020;50:472–84.
26. Lu S, Liu L, Demissie H, An G, Wang D. Design and application of metal-organic frameworks and derivatives as heterogeneous Fenton-like catalysts for organic wastewater treatment: a review. Environ Int. 2021;146: 106273.
27. Chen L, Zuo X, Yang S, Cai T, Ding D. Rational design and synthesis of hollow $Co_3O_4$@$Fe_2O_3$ core-shell nanostructure for the catalytic degradation of norfloxacin by coupling with peroxymonosulfate. Chem Eng J. 2019;359:373–84.
28. Tian D, Zhou H, Zhang H, Zhou P, You J, Yao G, Pan Z, Liu Y, Lai B. Heterogeneous photocatalyst-driven persulfate activation process under visible light irradiation: From basic catalyst design principles to novel enhancement strategies. Chem Eng J. 2022;428:131166.
29. Li Q, Liu J, Ren Z, Wang Z, Mao F, Wu H, Zhou R, Bu Y. Catalytic degradation of antibiotic by Co nanoparticles encapsulated in nitrogen-doped nanocarbon derived from Co-MOF for promoted peroxymonosulfate activation. Chem Eng J. 2022;429:132269.
30. Chen ML, Lu TH, Li SS, Wen L, Xu Z, Cheng YH. Photocatalytic degradation of imidacloprid by optimized Bi2WO6/NH2-MIL-88B(Fe) composite under visible light. Environ Sci Pollut Res. 2022;29:19583–93.
31. Wang Z, He M, Jiang H, He H, Qi J, Ma J. Photocatalytic MOF membranes with two-dimensional heterostructure for the enhanced removal of agricultural pollutants in water. Chem Eng J. 2022;435: 133870.
32. Yeganeh M, Farzadkia M, Jafari AJ, Sobhi HR, Esrafili A, Gholami M. Utilization of the copper recovered from waste printed circuit boards as a metal precursor for the synthesis of TiO2/magnetic-MOF(Cu) nanocomposite: application in photocatalytic degradation of pesticides in aquatic solutions. J Environ Manage. 2023;345: 118755.
33. Wu Q, Liu Y, Jing H, Yu H, Lu Y, Huo M, Huo H. Peculiar synergetic effect of γ-Fe2O3 nanoparticles and graphene oxide on MIL-53(Fe) for boosting photocatalysis. Chem Eng J. 2020;390: 124615.
34. Li X, Wang S, Xu B, Zhang X, Xu Y, Yu P, Sun Y. MOF etching-induced Co-doped hollow carbon nitride catalyst for efficient removal of antibiotic contaminants by enhanced perxymonosulfate activation. Chem Eng J. 2022;441: 136074.
35. Luo C, Lin Y, Zhang Y, Zhang S, Tong S, Wu S, Yang C. S-scheme heterojunction between MOFs and Ag3PO4 leads to efficient photodegradation of antibiotics in swine wastewater. Sep Purif Technol. 2023;320: 124052.
36. Zhang C, Li H, Li C, Li Z. Fe-Loaded MOF-545(Fe): peroxidase-like activity for dye degradation dyes and high adsorption for the removal of dyes from wastewater. Molecules. 2020;25:168.
37. Ge K, Hu Y, Li G. Surface initiated encapsulation of MOF-74 (Ni) on magnetic prickly-like nickel rods combined with silver nanoparticle decoration for simultaneous and selective surface-enhanced Raman spectroscopy analysis of T-2 and deoxynivalenol. Sens Actuator B-Chem. 2023;374: 132842.
38. Liu YQ, Song CG, Ding G, Yang J, Wu JR, Wu G, Zhang MZ, Song C, Guo LP, Qin JC, Yang YW. High-performance functional Fe-MOF for removing aflatoxin B1 and other organic pollutants. Adv Mater Interfaces. 2022;9:2102480.
39. Du Q, Zhang W, Xu N, Jiang X, Cheng J, Wang R, Wang P. Efficient and simultaneous removal of aflatoxin B1, B2, G1, G2, and zearalenone from vegetable oil by use of a metal–organic framework absorbent. Food Chem. 2023;418: 135881.
40. Yaghi O, Li G, Li H. Selective binding and removal of guests in a microporous metal–organic framework. Nature. 1995;378:703–6.
41. Yang FY, Du M, Yin KL, Qiu ZM, Zhao JW, Liu CL, Zhang GX, Gao YJ, Pang H. Applications of metal-organic frameworks in water treatment: a review. Small. 2022;18:2105715.
42. Xiao K, Shu B, Lv K, Huang P, Chang Q, Wu L, Wang S, Cao L. Recent progress of MIL MOF materials in degradation of organic pollutants by fenton reaction. Catalysts. 2023;13(4):734.
43. Dapaah MF, Niu Q, Yu Y, You T, Liu B, Cheng L. Efficient persistent organic pollutant removal in water using MIL-metal–organic framework driven Fenton-like reactions: a critical review. Chem Eng J. 2022;431:3.
44. Zou D, Liu D, Zhang J. From zeolitic imidazolate framework-8 to metal-organic frameworks (MOFs): representative substance for the general study of pioneering MOF applications. Energy Environ Mater. 2018;1(4):209–20.
45. Nguyen LTL, Le KKA, Phan NTS. A zeolite imidazolate framework ZIF-8 catalyst for friedel-crafts acylation. Chin J Catal. 2012;33:688–96.
46. Richelle MR, Mahaveer DK, Madhuprasad K. A comprehensive review on water remediation using UiO-66 MOFs and their derivatives. Chemosphere. 2022;302: 134845.
47. Ma S, Zhou H. A metal−organic framework with entatic metal centers exhibiting high gas adsorption affinity. J Am Chem Soc. 2006;128(36):11734–5.
48. Ma S, Sun D, Simmons JM, Collier CD, Yuan D, Zhou H. Metal-organic framework from an anthracene derivative containing nanoscopic cages exhibiting high methane uptake. J Am Chem Soc. 2008;130(3):1012–6.
49. Feng D, Gu Z, Chen Y, Park J, Wei Z, Sun Y, Bosch M, Yuan S, Zhou H. A highly stable porphyrinic zirconium metal-organic framework with shp-a topology. J Am Chem Soc. 2014;136(51):17714–7.
50. Liu Y, Howarth AJ, Hupp JT, Farha OK. Selective photooxidation of a mustard-gas simulant catalyzed by a porphyrinic metal-organic framework. Angew Chem Int Ed. 2015;54:9001–5.
51. Dapaah MF, Niu Q, Yu Y, You T, Liu B, Cheng L. Efficient persistent organic pollutant removal in water using MIL-metal–organic framework driven Fenton-like reactions: a critical review. Chem Eng J. 2022;431(3):134182.
52. Huang B, Li Y, Zeng W. Application status of zeolitic imidazolate framework in gas sensors. Nano Futures. 2022;6: 032003.
53. Cahn AF, Combs RL, Monzo EM, Prinslow SD, Harris CM, Penn RL. Onion-Like nanoparticles of the metal–organic framework UiO-66 synthesized by sequential spike crystal growth. J Cryst Growth. 2023;601: 126911.
54. Zeng Y, Ouyang Q, Yu Y, Tan L, Liu X, Zheng Y, Wu S. Defective homojunction porphyrin-based metal-organic frameworks for highly efficient sonodynamic therapy. Small Methods. 2023;7:2201248.
55. Al N, Amery HR, Abid S, Al-Saadi S, Wang SL. Facile directions for synthesis modification and activation of MOFs. Mater Today Chem. 2020;17:100343.
56. Abazari R, Mahjoub AR, Salehi G. Preparation of amine functionalized g-$C_3N_4$@(H/S)MOF NCs with visible light photocatalytic characteristic for 4-nitrophenol degradation from aqueous solution. J Hazard Mater. 2019;365:921–31.
57. Zhao ZH, Zheng K, Huang NY, Zhu HL, Huang JR, Liao PQ, Chen XM. A Cu(111)@metal-organic framework as a tandem catalyst for highly selective $CO_2$ electroreduction to $C_2H_4$. Chem Commun. 2021;57:12764–7.
58. Ma J, Wang S, He W, Chen H, Zhai X, Meng F, Fu Y. Synthesis of FeNiCo ternary hydroxides through green grinding method with metal-organic

frameworks as precursors for oxygen evolution reaction. Chemsuschem. 2021;14:5042–8.
59. Cui J, Liu T, Zhang Q, Wang T, Hou X. Rapid microwave synthesis of $Fe_3O_4$-PVP@ZIF-67 as highly effective peroxymonosulfate catalyst for degradation of bisphenol F and its mechanism analysis. Chem Eng J. 2021;404:126453.
60. Huang Z, Yu H, Wang L, Liu X, Lin T, Haq F, Vatsadze SZ, Lemenovskiy DA. Ferrocene-contained metal organic frameworks: from synthesis to applications. Coord Chem Rev. 2021;430:213737.
61. Li G, Yu K, Noordijk J, Meeusen-Wierts MHM, Gebben B, Oude Lohuis PAM, Schotman AHM, Bernaerts KV. Hydrothermal polymerization towards fully biobased polyazomethines. Chem Commun. 2020;56:9194–7.
62. Chen Y, Wu H, Yuan Y, Lv D, Xia Q. Highly rapid mechanochemical synthesis of a pillar-layer metal-organic framework for efficient $CH_4/N_2$ separation. Chem Eng J. 2020;385: 123836.
63. Crickmore TS, Sana HB, Mitchel HL, Clark M, Bradshaw D. Toward sustainable syntheses of Ca-based MOFs. Chem Commun. 2021;57:10592–5.
64. Kumar S, Jain S, Nehra M, Dilbaghi N, Marrazza G, Kim KH. Green synthesis of metal-organic frameworks: A state-of-the-art review of potential environmental and medical applications. Coord Chem Rev. 2020;420:213407.
65. Glowniak S, Szczesniak B, Choma J, Jaroniec M. Advances in microwave synthesis of nanoporous materials. Adv Mater. 2021;33: e2103477.
66. Li Q, Liu Y, Niu S, Li C, Chen C, Liu Q, Huo J. Microwave-assisted rapid synthesis and activation of ultrathin trimetal-organic framework nanosheets for efficient electrocatalytic oxygen evolution. J Colloid Interface Sci. 2021;603:148–56.
67. Jhung SH, Lee JH, Yoon JW, Serre C, Férey G, Chang JS. Microwave synthesis of chromium terephthalate MIL-101 and its benzene sorption ability. Adv Mater. 2007;19:121–4.
68. Vo TK, Kim J, Vu TH, Nguyen VC, Quang DT. Creating Cu(I)-decorated defective UiO-66(Zr) framework with high CO adsorption capacity and selectivity. Sep Purif Technol. 2022;283:120237.
69. Hillman F, Zimmerman JM, Paek SM, Hamid MRA, Lim WT, Jeong HK. Rapid microwave-assisted synthesis of hybrid zeolitic-imidazolate frameworks with mixed metals and mixed linkers. J Mater Chem A. 2017;5:6090–9.
70. Li J, Zhao Y, Wang X, Wang T, Hou X. Rapid microwave synthesis of PCN-134–2D for singlet oxygen based-oxidative degradation of ranitidine under visible light: mechanism and toxicity assessment. Chem Eng J. 2022;443:136424.
71. Mahringer A, Doblinger M, Hennemann M, Gruber C, Fehn D, Scheurle PI, Hosseini P, Santourian I, Schirmacher A, Rotter JM, Wittstock G, Meyer K, Clark T, Bein T, Medina DD. An electrically conducting three-dimensional iron-catecholate porous framework. Angew Chem-Int Edit. 2021;60:18065–72.
72. Vo TK, Kim J, Vu TH, Nguyen VC, Quang DT. Creating Cu(I)-decorated defective UiO-66(Zr) framework with high CO adsorption capacity and selectivity. Sep Purif Technol. 2022;283: 120237.
73. Yi B, Zhao H, Cao L, Si X, Jiang Y, Cheng P, Zuo Y, Zhang Y, Su L, Wang Y, Tsung CK, Chou LY, Xie J. A direct mechanochemical conversion of Pt-doped metal-organic framework-74 from doped metal oxides for CO oxidation. Mater Today Nano. 2022;17:100158.
74. Abuzalat O, Wong D, Elsayed M, Park S, Kim S. Sonochemical fabrication of Cu(II) and Zn(II) metal-organic framework films on metal substrates. Ultrason Sonochem. 2018;45:180–8.
75. Liu Y, Wei Y, Liu M, Bai Y, Wang X, Shang S, Chen J, Liu Y. Electrochemical synthesis of large area two-dimensional metal-organic framework films on copper anodes. Angew Chem-Int Edit. 2021;60:2887–91.
76. Ardila-Fierro KJ, Hernandez JG. Sustainability assessment of mechanochemistry by using the twelve principles of green chemistry. Chemsuschem. 2021;14:2145–62.
77. Huskić I, Lennox CB, Friščić T. Accelerated ageing reactions: Towards simpler, solvent-free, low energy chemistry. Green Chem. 2020;22:5881–901.
78. Peng L, Zhang J, Xue Z, Han B, Sang X, Liu C, Yang G. Highly mesoporous metal-organic framework assembled in a switchable solvent. Nat Commun. 2014;5:4465.
79. Friščić T. New opportunities for materials synthesis using mechanochemistry. J Mater Chem. 2010;20:7599–605.
80. Uzarevic K, Wang TC, Moon SY, Fidelli AM, Hupp JT, Farha OK, Friscic T. Mechanochemical and solvent-free assembly of zirconium-based metal-organic frameworks. Chem Commun. 2016;52:2133–6.
81. Vaitsis C, Sourkouni G, Argirusis C. Metal organic frameworks (MOFs) and ultrasound: a review. Ultrason Sonochem. 2019;52:106–19.
82. Zarekarizi F, Morsali A. Ultrasonic-assisted synthesis of nano-sized metal-organic framework; a simple method to explore selective and fast Congo Red adsorption. Ultrason Sonochem. 2020;69: 105246.
83. Armstrong MR, Senthilnathan S, Balzer CJ, Shan B, Chen L, Mu B. Particle size studies to reveal crystallization mechanisms of the metal organic framework HKUST-1 during sonochemical synthesis. Ultrason Sonochem. 2017;34:365–70.
84. Fu J, Wu YN. A showcase of green chemistry: Sustainable synthetic approach of zirconium-based MOF materials. Chem-Eur J. 2021;27:9967–87.
85. Ren H, Wei T. Electrochemical synthesis methods of metal-organic frameworks and their environmental analysis applications: a review. ChemElectroChem. 2022;9:e202200196.
86. Thorne MF, Gómez MLR, Bumstead AM, Li S, Bennett TD. Mechanochemical synthesis of mixed metal, mixed linker, glass-forming metal-organic frameworks. Green Chem. 2020;22:2505–12.
87. Aris AZ, Mohd Hir ZA, Razak MR. Metal-organic frameworks (MOFs) for the adsorptive removal of selected endocrine disrupting compounds (EDCs) from aqueous solution: A review. Appl Mater Today. 2020;21:100796.
88. Sukatis FF, Wee SY, Aris AZ. Potential of biocompatible calcium-based metal-organic frameworks for the removal of endocrine-disrupting compounds in aqueous environments. Water Res. 2022;218: 118406.
89. Gao Y, Kang R, Xia J, Yu G, Deng S. Understanding the adsorption of sulfonamide antibiotics on MIL-53s: Metal dependence of breathing effect and adsorptive performance in aqueous solution. J Colloid Interface Sci. 2019;535:159–68.
90. Zhao X, Zhao H, Dai W, Wei Y, Wang Y, Zhang Y, Zhi L, Huang H, Gao Z. A metal-organic framework with large 1-D channels and rich OH sites for high-efficiency chloramphenicol removal from water. J Colloid Interface Sci. 2018;526:28–34.
91. Zhang J, Xiang S, Wu P, Wang D, Lu S, Wang S, Gong F, Wei X, Ye X, Ding P. Recent advances in performance improvement of metal-organic frameworks to remove antibiotics: Mechanism and evaluation. Sci Total Environ. 2022;811: 152351.
92. Yu J, Xiong W, Li X, Yang Z, Cao J, Jia M, Xu R, Zhang Y. Functionalized MIL-53(Fe) as efficient adsorbents for removal of tetracycline antibiotics from aqueous solution. Microporous Mesoporous Mat. 2019;290:109642.
93. Dehghan A, Zarei A, Jaafari J, Shams M, Mousavi Khaneghah A. Tetracycline removal from aqueous solutions using zeolitic imidazolate frameworks with different morphologies: a mathematical modeling. Chemosphere. 2019;217:250–60.
94. Yang ZH, Cao J, Chen YP, Li X, Xiong WP, Zhou YP, Zhou CP, Xu R, Zhang YR. Mn-doped zirconium metal-organic framework as an effective adsorbent for removal of tetracycline and Cr(VI) from aqueous solution. Microporous Mesoporous Mat. 2019;277:277–85.
95. Jin J, Yang Z, Xiong W, Zhou Y, Xu R, Zhang Y, Cao J, Li X, Zhou C. Cu and Co nanoparticles co-doped MIL-101 as a novel adsorbent for efficient removal of tetracycline from aqueous solutions. Sci Total Environ. 2019;650:408–18.
96. Jin Y, Mi X, Qian J, Ma N, Dai W. Modular Construction of an MIL-101(Fe)@MIL-100(Fe) Dual-Compartment Nanoreactor and Its Boosted Photocatalytic Activity toward Tetracycline. ACS Appl Mater Interfaces. 2022;14(42):48285–95.
97. Li W, Wu X, Li S, Tang W, Chen Y. Magnetic porous $Fe_3O_4$/carbon octahedra derived from iron-based metal-organic framework as heterogeneous Fenton-like catalyst. Appl Surf Sci. 2018;436:252–62.
98. Guo Y, Qin X, Tang Y, Ma Q, Zhang J, Zhao L. CotA laccase, a novel aflatoxin oxidase from Bacillus licheniformis, transforms aflatoxin B1 to aflatoxin Q1 and epi-aflatoxin Q1. Food Chem. 2020;325: 126877.
99. Loi M, Fanelli F, Zucca P, Liuzzi VC, Quintieri L, Cimmarusti MT, Monaci L, Haidukowski M, Logrieco AF, Sanjust E, Mule G. Aflatoxin B(1) and M(1)

degradation by Lac2 from pleurotus pulmonarius and redox mediators. Toxins. 2016;8:245.
100. Ai Y, Hu ZN, Liang X, Sun HB, Xin H, Liang Q. Recent advances in nanozymes: From matters to bioapplications. Adv Funct Mater. 2021;32(14):2110432.
101. Zhang X, Lin S, Liu S, Tan X, Dai Y, Xia F. Advances in organometallic/organic nanozymes and their applications. Coord Chem Rev. 2021;429:213652.
102. Liang S, Wu XL, Xiong J, Zong MH, Lou WY. Metal-organic frameworks as novel matrices for efficient enzyme immobilization: an update review. Coord Chem Rev. 2020;406:213149.
103. Liu DM, Chen J, Shi YP. Advances on methods and easy separated support materials for enzymes immobilization. TrAC-Trends Anal Chem. 2018;102:332–42.
104. Zhang X, Tu R, Lu Z, Peng J, Hou C, Wang Z. Hierarchical mesoporous metal-organic frameworks encapsulated enzymes: Progress and perspective. Coord Chem Rev. 2021;443:214032.
105. Metzger KE, Moyer MM, Trewyn BG. Tandem catalytic systems integrating biocatalysts and inorganic catalysts using functionalized porous materials. ACS Catal. 2020;11:110–22.
106. Cui J, Ren S, Sun B, Jia S. Optimization protocols and improved strategies for metal-organic frameworks for immobilizing enzymes: current development and future challenges. Coord Chem Rev. 2018;370:22–41.
107. Raja DS, Liu WL, Huang HY, Lin CH. Immobilization of protein on nanoporous metal-organic framework materials. Comments Inorganic Chem. 2015;35:331–49.
108. Liu X, Qi W, Wang Y, Lin D, Yang X, Su R, He Z. Rational design of mimic multienzyme systems in hierarchically porous biomimetic metal-organic frameworks. ACS Appl Mater Inter. 2018;10:33407–15.
109. Jung S, Kim Y, Kim SJ, Kwon TH, Huh S, Park S. Bio-functionalization of metal-organic frameworks by covalent protein conjugation. Chem Commun. 2011;47:2904–6.
110. Li P, Moon SY, Guelta MA, Harvey SP, Hupp JT, Farha OK. Encapsulation of a nerve agent detoxifying enzyme by a mesoporous zirconium metal-organic framework engenders thermal and long-term stability. J Am Chem Soc. 2016;138:8052–5.
111. Zhang R, Wang L, Han J, Wu J, Li C, Ni L, Wang Y. Improving laccase activity and stability by HKUST-1 with cofactor via one-pot encapsulation and its application for degradation of bisphenol A. J Hazard Mater. 2020;383: 121130.
112. Xue S, Li J, Zhou L, Gao J, Liu G, Ma L, He Y, Jiang Y. Simple Purification and immobilization of His-tagged organophosphohydrolase from cell culture supernatant by metal organic frameworks for degradation of organophosphorus pesticides. J Agric Food Chem. 2019;67:13518–25.
113. Li SF, Zhai XJ, Zhang C, Mo HL, Zang SQ. Enzyme immobilization in highly ordered macro-microporous metal-organic frameworks for rapid biodegradation of hazardous dyes. Inorg Chem Front. 2020;7:3146–53.
114. Wang Z, Sun Y. A hybrid nanobiocatalyst with in situ encapsulated enzyme and exsolved Co nanoclusters for complete chemoenzymatic conversion of methyl parathion to 4-aminophenol. J Hazard Mater. 2022;424: 127755.
115. Ali A, Ovais M, Zhou H, Rui Y, Chen C. Tailoring metal-organic frameworks-based nanozymes for bacterial theranostics. Biomaterials. 2021;275: 120951.
116. Huang X, Zhang S, Tang Y, Zhang X, Bai Y, Pang H. Advances in metal-organic framework-based nanozymes and their applications. Coord Chem Rev. 2021;449:214216.
117. Feng D, Gu ZY, Li JR, Jiang HL, Wei Z, Zhou HC. Zirconium-metalloporphyrin PCN-222: mesoporous metal-organic frameworks with ultrahigh stability as biomimetic catalysts. Angew Chem-Int Edit. 2012;51:10307–10.
118. Li S, Hou Y, Chen Q, Zhang X, Cao H, Huang Y. Promoting active sites in MOF-derived homobimetallic hollow nanocages as a high-performance multifunctional nanozyme catalyst for biosensing and organic pollutant degradation. ACS Appl Mater Inter. 2020;12:2581–90.
119. He J, Zhang Y, Zhang X, Huang Y. Highly efficient Fenton and enzyme-mimetic activities of $NH_2$-MIL-88B(Fe) metal organic framework for methylene blue degradation. Sci Rep. 2018;8:5159.
120. Zhong Y, Wang T, Lao Z, Lu M, Liang S, Cui X, Li QL, Zhao S. Au-Au/$IrO_2$@Cu(PABA) reactor with tandem enzyme-mimicking catalytic activity for organic dye degradation and antibacterial application. ACS Appl Mater Inter. 2021;13:21680–92.
121. Fu T, Xu C, Guo R, Lin C, Huang Y, Tang Y, Wang H, Zhou Q, Lin Y. Zeolitic imidazolate framework-90 nanoparticles as nanozymes to mimic organophosphorus hydrolase. ACS Appl Nano Mater. 2021;4:3345–50.
122. Ong CB, Ng LY, Mohammad AW. A review of ZnO nanoparticles as solar photocatalysts: Synthesis, mechanisms and applications. Renew Sust Energ Revi. 2018;81:536–51.
123. Zhou C, Lai C, Huang D, Zeng G, Zhang C, Cheng M, Hu L, Wan J, Xiong W, Wen M, Wen X, Qin L. Highly porous carbon nitride by supramolecular preassembly of monomers for photocatalytic removal of sulfamethazine under visible light driven. Appl Catal B-Environ. 2018;220:202–10.
124. Wang CC, Yi XH, Wang P. Powerful combination of MOFs and $C_3N_4$ for enhanced photocatalytic performance. Appl Catal B-Environ. 2019;247:24–48.
125. Luo H, Zeng Z, Zeng G, Zhang C, Xiao R, Huang D, Lai C, Cheng M, Wang W, Xiong W, Yang Y, Qin L, Zhou C, Wang H, Zhou Y, Tian S. Recent progress on metal-organic frameworks based- and derived-photocatalysts for water splitting. Chem Eng J. 2020;383:123196.
126. Andersen J, Han C, O'Shea K, Dionysiou DD. Revealing the degradation intermediates and pathways of visible light-induced NF-$TiO_2$ photocatalysis of microcystin-LR. Appl Catal B-Environ. 2014;154–155:259–66.
127. Tang R, Gong D, Zhou Y, Deng Y, Feng C, Xiong S, Huang Y, Peng G, Li L, Zhou Z. Unique g-$C_3N_4$/PDI-g-$C_3N_4$ homojunction with synergistic piezo-photocatalytic effect for aquatic contaminant control and $H_2O_2$ generation under visible light. Appl Catal B-Environ. 2022;303:120929.
128. Singh A, Singh AK, Liu J, Kumar A. Syntheses, design strategies, and photocatalytic charge dynamics of metal-organic frameworks (MOFs): a catalyzed photo-degradation approach towards organic dyes. Catal Sci Technol. 2021;11:3946–89.
129. Zhan W, Sun L, Han X. Recent progress on engineering highly efficient porous semiconductor photocatalysts derived from metal-organic frameworks. Nano-Micro Lett. 2019;11:1.
130. Chen H, Yuan X, Jiang L, Wang H, Yu H, Wang X. Intramolecular modulation of iron-based metal organic framework with energy level adjusting for efficient photocatalytic activity. Appl Catal B-Environ. 2022;302:120823.
131. Zhu J, Li PZ, Guo W, Zhao Y, Zou R. Titanium-based metal-organic frameworks for photocatalytic applications. Coord Chem Rev. 2018;359:80–101.
132. Feng H, Li H, Liu X, Huang Y, Pan Q, Peng R, Du R, Zheng X, Yin Z, Li S, He Y. Porphyrin-based Ti-MOFs conferred with single-atom Pt for enhanced photocatalytic hydrogen evolution and NO removal. Chem Eng J. 2022;428:132045.
133. Lü CX, Zhan GP, Chen K, Liu ZK, Wu CD. Anchoring Zn-phthalocyanines in the pore matrices of UiO-67 to improve highly the photocatalytic oxidation efficiency. Appl Catal B-Environ. 2020;279:119350.
134. Hai G, Wang H. Theoretical studies of metal-organic frameworks: calculation methods and applications in catalysis, gas separation, and energy storage. Coord Chem Rev. 2022;469: 214670.
135. Fatima R, Kim JO. Inhibiting photocatalytic electron-hole recombination by coupling MIL-125(Ti) with chemically reduced, nitrogen-containing graphene oxide. Appl Surf Sci. 2021;541:119350.
136. Li YX, Wang X, Wang CC, Fu H, Liu Y, Wang P, Zhao C. S-$TiO_2$/UiO-66-$NH_2$ composite for boosted photocatalytic Cr(VI) reduction and bisphenol A degradation under LED visible light. J Hazard Mater. 2020;399: 123085.
137. Jin P, Wang L, Ma X, Lian R, Huang J, She H, Zhang M, Wang Q. Construction of hierarchical $ZnIn_2S_4$@PCN-224 heterojunction for boosting photocatalytic performance in hydrogen production and degradation of tetracycline hydrochloride. Appl Catal B-Environ. 2021;284:119762.
138. Yao P, Liu H, Wang D, Chen J, Li G, An T. Enhanced visible-light photocatalytic activity to volatile organic compounds degradation and deactivation resistance mechanism of titania confined inside a metal-organic framework. J Colloid Interface Sci. 2018;522:174–82.
139. Li X, Le Z, Chen X, Li Z, Wang W, Liu X, Wu A, Xu P, Zhang D. Graphene oxide enhanced amine-functionalized titanium metal organic framework for visible-light-driven photocatalytic oxidation of gaseous pollutants. Appl Catal B-Environ. 2018;236:501–8.
140. Huang J, Zhang X, Song H, Chen C, Han F, Wen C. Protonated graphitic carbon nitride coated metal-organic frameworks with enhanced

visible-light photocatalytic activity for contaminants degradation. Appl Surf Sci. 2018;441:85–98.
141. Zhang Y, Zhou J, Feng Q, Chen X, Hu Z. Visible light photocatalytic degradation of MB using UiO-66/g-$C_3N_4$ heterojunction nanocatalyst. Chemosphere. 2018;212:523–32.
142. Chen DM, Liu XH, Zhang NN, Liu CS, Du M. Immobilization of polyoxometalate in a cage-based metal-organic framework towards enhanced stability and highly effective dye degradation. Polyhedron. 2018;152:108–13.
143. Wang S, Meng F, Sun X, Bao M, Ren J, Yu S, Zhang Z, Ke J, Zeng L. Bimetallic Fe/In metal-organic frameworks boosting charge transfer for enhancing pollutant degradation in wastewater. Appl Surf Sci. 2020;528:147053.
144. Zhao Y, Dong Y, Lu F, Ju C, Liu L, Zhang J, Zhang B, Feng Y. Coordinative integration of a metal-porphyrinic framework and $TiO_2$ nanoparticles for the formation of composite photocatalysts with enhanced visible-light-driven photocatalytic activities. J Mater Chem A. 2017;5:15380–9.
145. Gao Y, Xia J, Liu D, Kang R, Yu G, Deng S. Synthesis of mixed-linker Zr-MOFs for emerging contaminant adsorption and photodegradation under visible light. Chem Eng J. 2019;378:122118.
146. Chen SS, Hu C, Liu CH, Chen YH, Ahamad T, Alshehri SM, Huang PH, Wu KC. De Novo synthesis of platinum-nanoparticle-encapsulated UiO-66-$NH_2$ for photocatalytic thin film fabrication with enhanced performance of phenol degradation. J Hazard Mater. 2020;397: 122431.
147. Liu C, Bao T, Yuan L, Zhang C, Wang J, Wan J, Yu C. Semiconducting MOF@ZnS heterostructures for photocatalytic hydrogen peroxide production: Heterojunction coverage matters. Adv Funct Mater. 2021;32:2111404.
148. Li L, Yu X, Xu L, Zhao Y. Fabrication of a novel type visible-light-driven heterojunction photocatalyst: Metal-porphyrinic metal organic framework coupled with $PW_{12}/TiO_2$. Chem Eng J. 2020;386:123955.
149. Liang Q, Gao W, Liu C, Xu S, Li Z. A novel 2D/1D core-shell heterostructures coupling MOF-derived iron oxides with $ZnIn_2S_4$ for enhanced photocatalytic activity. J Hazard Mater. 2020;392: 122500.
150. Li Y, Fang Y, Cao Z, Li N, Chen D, Xu Q, Lu J. Construction of g-$C_3N_4$/PDI@MOF heterojunctions for the highly efficient visible light-driven degradation of pharmaceutical and phenolic micropollutants. Appl Catal B-Environ. 2019;250:150–62.
151. Sharma VK, Feng M. Water depollution using metal-organic frameworks-catalyzed advanced oxidation processes: A review. J Hazard Mater. 2019;372:3–16.
152. Z. Lu, X. Cao, H. Wei, W. Huo, Q. Wang, K. Li, Strong enhancement effect of bisulfite on MIL-68(Fe)-catalyzed Fenton-like reaction for organic pollutants degradation, Appl. Surf. Sci. **542** (2021)
153. Cheng M, Lai C, Liu Y, Zeng G, Huang D, Zhang C, Qin L, Hu L, Zhou C, Xiong W. Metal-organic frameworks for highly efficient heterogeneous Fenton-like catalysis. Coord Chem Rev. 2018;368:80–92.
154. Yang J, Zeng D, Li J, Dong L, Ong WJ, He Y. A highly efficient Fenton-like catalyst based on isolated diatomic Fe-Co anchored on N-doped porous carbon. Chem Eng J. 2021;404:126376.
155. Xu W, Xue W, Huang H, Wang J, Zhong C, Mei D. Morphology controlled synthesis of α-$Fe_2O_3$-x with benzimidazole-modified Fe-MOFs for enhanced photo-Fenton-like catalysis. Appl Catal B-Environ. 2021;291:120129.
156. Wang L, Jin P, Duan S, Huang J, She H, Wang Q, T. An, Accelerated Fenton-like kinetics by visible-light-driven catalysis over iron(iii) porphyrin functionalized zirconium MOF: effective promotion on the degradation of organic contaminants. Environ Sci-Nano. 2019;6:2652–3266.
157. Liu H, Yin H, Zhu M, Dang Z. Degradation of organophosphorus flame retardants in heterogeneous photo-Fenton system driven by Fe(III)-based metal organic framework: Intermediates and their potential interference on bacterial metabolism. Chemosphere. 2022;291: 133072.
158. Xing DN, Cui ZH, Liu YY, Wang ZY, Wang P, Zheng ZK, Cheng HF, Dai Y, Huang BB. Two-dimensional π-d conjugated metal-organic framework Fe-3(hexaiminotriphenylene)(2) as a photo-Fenton like catalyst for highly efficient degradation of antibiotics. Appl Catal B-Environ. 2021;290: 120029.
159. Du X, Oturan MA, Zhou M, Belkessa N, Su P, Cai J, Trellu C, Mousset E. Nanostructured electrodes for electrocatalytic advanced oxidation processes: from materials preparation to mechanisms understanding and wastewater treatment applications. Appl Catal B-Environ. 2021;296: 120332.
160. Wu D, Hua T, Han S, Lan X, Cheng J, Wen W, Hu Y. Two-dimensional manganese-iron bimetallic MOF-74 for electro-Fenton degradation of sulfamethoxazole. Chemosphere. 2023;327: 138514.
161. Huang S, Wang Y, Qiu S, Wan J, Ma Y, Yan Z, Xie Q. In-situ fabrication from MOFs derived $Mn_xCo_{3-x}$@C modified graphite felt cathode for efficient electro-Fenton degradation of ciprofloxacin. Appl Surf Sci. 2022;586: 152804.
162. Ye Z, Schukraft GEM, L'Hermitte A, Xiong Y, Brillas E, Petit C, Sirés I. Mechanism and stability of an Fe-based 2D MOF during the photoelectro-Fenton treatment of organic micropollutants under UVA and visible light irradiation. Water Res. 2020;184: 115986.
163. Li Y, Li X, Wang B. Constructing tunable coordinatively unsaturated sites in Fe-based metal-organic framework for effective degradation of pharmaceuticals in water: Performance and mechanism. Chemosphere. 2023;310: 136816.
164. Song Q, Li Y, Xie W, Gao C, Liu L, Liu B. Catalytic degradation of carbamazepine by metal organic frameworks (MOFs) derived magnetic catalyst Fe@PC in an electro-Fenton coupled membrane filtration system: performance, pathway, and mechanism. Sep Purif Technol. 2023;309: 122988.
165. Xiong Z, Jiang Y, Wu Z, Yao G, Lai B. Synthesis strategies and emerging mechanisms of metal-organic frameworks for sulfate radical-based advanced oxidation process: a review. Chem Eng J. 2021;421(2):127863.
166. Han MS, Zhu WK, Hossain MSA, You J, Kim J. Recent progress of functional metal-organic framework materials for water treatment using sulfate radicals. Environ Res. 2022;211:112956.
167. Liu N, Lu N, Yu H, Chen S, Quan X. Degradation of aqueous bisphenol A in the CoCN/Vis/PMS system: catalyst design, reaction kinetic and mechanism analysis. Chem Eng J. 2021;407:127228.
168. Roy D, Neogi S, De S. Visible light assisted activation of peroxymonosulfate by bimetallic MOF based heterojunction MIL-53(Fe/Co)/$CeO_2$ for atrazine degradation: Pivotal roles of dual redox cycle for reactive species generation. Chem Eng J. 2022;430:133069.
169. Duan MJ, Guan ZY, Ma YW, Wan JQ, Wang Y, Qu YF. A novel catalyst of MIL-101(Fe) doped with Co and Cu as persulfate activator: synthesis, characterization, and catalytic performance. Chem. 2018;72:235–50.
170. Arulpriya P, Krishnaveni T, Shanmugasundaram T, Kadirvelu K. Mesoporous $TiO_2$ @ Fe metal organic framework nanocomposite for an efficient chlorpyrifos detection and degradation. J Ind Eng Chem. 2022;112:146–61.
171. Xu M, Wang J, Liang X, Fang W, Zhu C, Wang F. MOF-derived $ZrO_2$-C nanoparticles modified $PbO_2$ electrode for high-efficiency electrocatalytic degradation of nitrophenolic compounds in wastewater. Sep Purif Technol. 2023;318: 123921.
172. Onfray CC, Rojas S, Zanoni MVB, Salazar R. An updated review of metal–organic framework materials in photo(electro)catalytic applications: From $CO_2$ reduction to wastewater treatments. Curr Opin Electrochem. 2021;26: 100669.
173. Jia M, Yang Z, Xu H, Song P, Xiong W, Cao J, Zhang Y, Xiang Y, Hu J, Zhou C, Yang Y, Wang W. Integrating N and F co-doped $TiO_2$ nanotubes with ZIF-8 as photoelectrode for enhanced photo-electrocatalytic degradation of sulfamethazine. Chem Eng J. 2020;388: 124388.
174. González AS, Martínez SS. Study of the sonophotocatalytic degradation of basic blue 9 industrial textile dye over slurry titanium dioxide and influencing factors. Ultrason Sonochem. 2008;15:1038–42.
175. Mosleh S, Rezaei K, Dashtian K, Salehi Z. Ce/Eu redox couple functionalized HKUST-1 MOF insight to sono-photodegradation of malathion. J Hazard Mater. 2021;409: 124478.
176. Sajjadi S, Khataee A, Bagheri N, Kobya M, Şenocak A, Demirbas E, Karaoğlu AG. Degradation of diazinon pesticide using catalyzed persulfate with $Fe_3O_4$@MOF-2 nanocomposite under ultrasound irradiation. J Ind Eng Chem. 2019;77:280–90.
177. Durán A, Monteagudo JM, Sanmartín I, García-Díaz A. Sonophotocatalytic mineralization of antipyrine in aqueous solution. Appl Catal B-Environ. 2013;138–139:318–25.
178. Luo X, Huang G, Chen X, Guo J, Yang W, Tang W, Yue T, Li Z. Ingenious ambient temperature fabrication zirconium-metal organic framework

laden polysaccharide aerogel as an efficient glyphosate scavenger. J Environ Chem Eng. 2021;9:106808.
179. Peng H, Xiong W, Yang Z, Xu Z, Cao J, Jia M, Xiang Y. Advanced MOFs@aerogel composites: construction and application towards environmental remediation. J Hazard Mater. 2022;432: 128684.
180. Chen MM, Niu HY, Niu CG, Guo H, Liang S, Yang YY. Metal-organic framework-derived CuCo/carbon as an efficient magnetic heterogeneous catalyst for persulfate activation and ciprofloxacin degradation. J Hazard Mater. 2022;424: 127196.
181. Yang R, Peng Q, Yu B, Shen Y, Cong H. Yolk-shell $Fe_3O_4$@MOF-5 nanocomposites as a heterogeneous Fenton-like catalyst for organic dye removal. Sep Purif Technol. 2021;267:118620.
182. Zhu H, Yang X, Cranston ED, Zhu S. Flexible and porous nanocellulose aerogels with high loadings of metal-organic-framework particles for separations applications. Adv Mater. 2016;28:7652–7.
183. Zhao G, Zhao H, Shi L, Cheng B, Xu X, Zhuang X. A highly efficient adsorbent constructed by the in situ assembly of Zeolitic imidazole framework-67 on 3D aramid nanofiber aerogel scaffold. Sep Purif Technol. 2021;274:119054.
184. Wang C, Wang H, Luo R, Liu C, Li J, Sun X, Shen J, Han W, Wang L. Metal-organic framework one-dimensional fibers as efficient catalysts for activating peroxymonosulfate. Chem Eng J. 2017;330:262–71.
185. Li Y, He Y, Zhuang J, Shi H. Hierarchical microsphere encapsulated in graphene oxide composite for durable synergetic membrane separation and Fenton-like degradation. Chem Eng J. 2022;430:133124.
186. He Y, Fu Q, Li X, Yin L, Wang D, Liu Y. ZIF-8-derived photocatalyst membrane for water decontamination: from static adsorption-degradation to dynamic flow removal. Sci Total Environ. 2022;824: 153865.
187. Ren W, Gao J, Lei C, Xie Y, Cai Y, Ni Q, Yao J. Recyclable metal-organic framework/cellulose aerogels for activating peroxymonosulfate to degrade organic pollutants. Chem Eng J. 2018;349:766–74.
188. Ren Y, Hersch SJ, He X, Zhou R, Dong TG, Lu Q. A lightweight, mechanically strong, and shapeable copper-benzenedicarboxylate/cellulose aerogel for dye degradation and antibacterial applications. Sep Purif Technol. 2022;283:120229.
189. He D, Niu H, He S, Mao L, Cai Y, Liang Y. Strengthened Fenton degradation of phenol catalyzed by core/shell Fe–Pd@C nanocomposites derived from mechanochemically synthesized Fe-Metal organic frameworks. Water Res. 2019;162:151–60.
190. Zhang X, Lin B, Li X, Wang X, Huang K, Chen Z. MOF-derived magnetically recoverable Z-scheme ZnFe2O4/Fe2O3 perforated nanotube for efficient photocatalytic ciprofloxacin removal. Chem Eng J. 2022;430(1):132728.
191. Pu M, Wan J, Zhang F, Brusseau ML, Ye D, Niu J. Insight into degradation mechanism of sulfamethoxazole by metal-organic framework derived novel magnetic Fe@C composite activated persulfate. J Hazard Mater. 2021;414: 125598.
192. Zhao S, Li S, Long YE, Shen X, Zhao Z, Wei Q, Wang S, Zhang Z, Zhang X, Zhang Z. Ce-based heterogeneous catalysts by partial thermal decomposition of Ce-MOFs in activation of peroxymonosulfate for the removal of organic pollutants under visible light. Chemosphere. 2021;280:130637.
193. Jhinjer HS, Singh A, Bhattacharya S, Jassal M, Agrawal AK. Metal-organic frameworks functionalized smart textiles for adsorptive removal of hazardous aromatic pollutants from ambient air. J Hazard Mater. 2021;411: 125056.
194. Yoo DK, Woo HC, Jhung SH. Removal of particulate matters with isostructural Zr-based metal-organic frameworks coated on cotton: Effect of porosity of coated MOFs on removal. ACS Appl Mater Inter. 2020;12:34423–31.
195. Tahazadeh S, Mohammadi T, Tofighy MA, Khanlari S, Karimi H, Motejadded Emrooz HB. Development of cellulose acetate/metal-organic framework derived porous carbon adsorptive membrane for dye removal applications. J Membr Sci. 2021;638:119692.
196. Seo JY, Song Y, Lee JH, Kim H, Cho S, Baek KY. Robust nanocellulose/metal-organic framework aerogel composites: Superior performance for static and continuous disposal of chemical warfare agent simulants. ACS Appl Mater Inter. 2021;13:33516–23.

## Publisher's Note